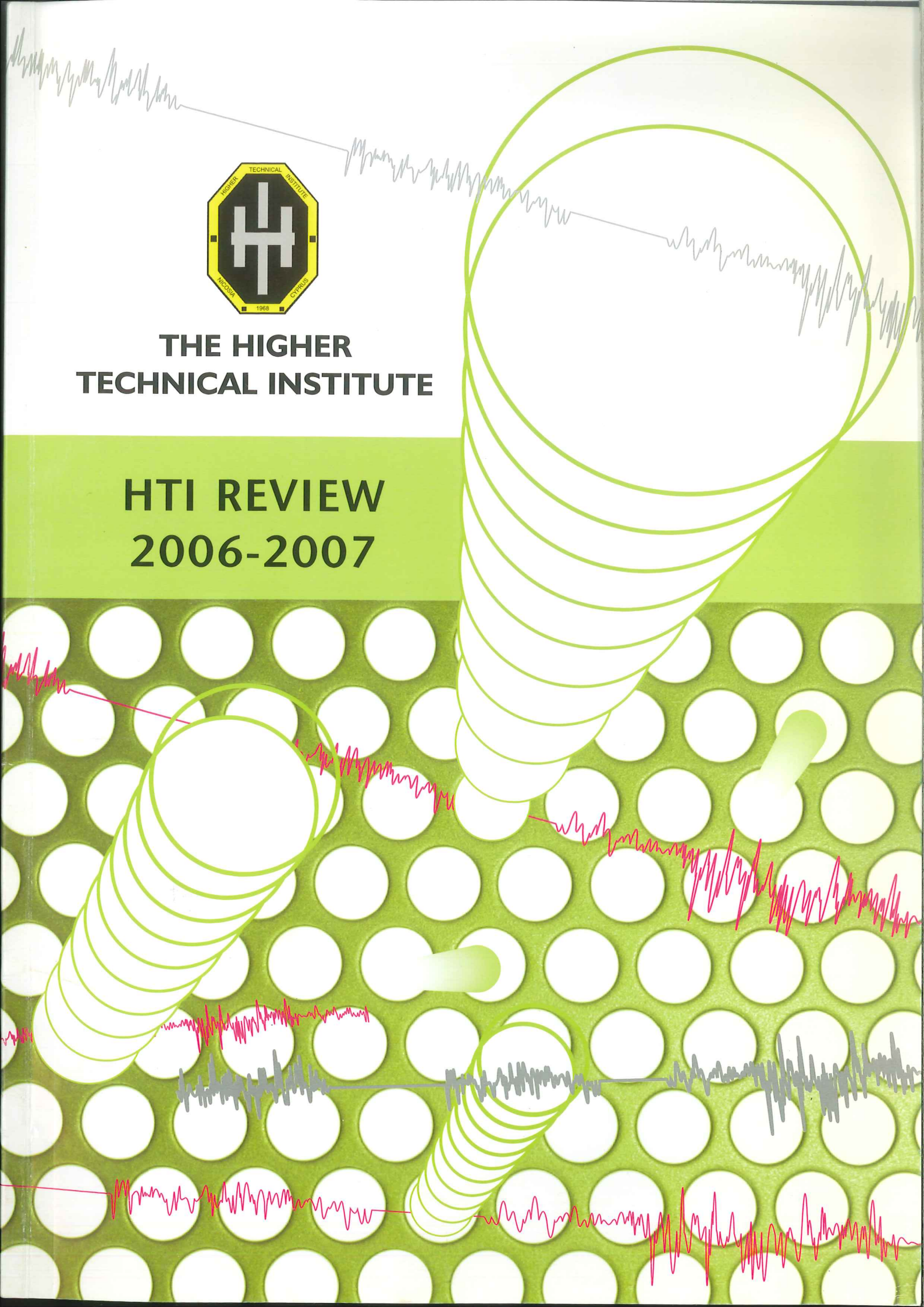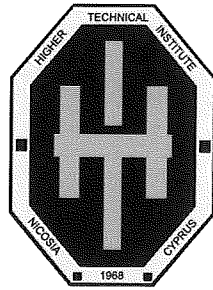# THE HIGHER TECHNICAL INSTITUTE

HTI REVIEW
2006-2007

THE HIGHER
TECHNICAL INSTITUTE

THE HIGHER TECHNICAL INSTITUTE REVIEW 2006-2007

No 36, November 2007, Nicosia - Cyprus

CONTENTS

FROM THE
EDITORS' DESK...

Dear Readers,

Welcome to the latest edition of the HTI Review. The HTI Review has become a tradition since 1971 and has been ever since a means of expressing our research interests and sharing our thoughts, views, findings on a wide spectrum of fields.

As a tertiary education institution, the HTI encourages its staff to be involved in research and welcomes any productive and thorough investigation of topics which fall under their areas of interest. At the HTI the emphasis is placed on both teaching and instructing the students as well as the personal research development of the staff.

This is illustrated by the wide participation of staff in various courses, seminars, visits in Cyprus and abroad, as well as the attendance of staff in a number of educational European programmes such as the Socrates, Erasmus and Leonardo DaVinci.

In this issue, articles covering the areas of technology, technical language teaching and others add up to a fascinating collection.

We hope that reading the material presented in this issue will prove to be a fruitful experience which will provide you with interesting information and will initiate discussion and further research in the same or related areas. After all, this is what an academic institution should do: create the means and opportunities where ideas and experiences from widely differing contexts can be brought together and be exchanged.

Although HTI is currently undergoing a major transitional period and the future of the Institute is still under discussion what is most definitely certain and unchangeable is the undiminished determination and eagerness of the staff to continue their research and further development. Regardless of what the future may hold, everybody here at the Institute pledges to maintain the high standard of teaching and research and to make a valuable contribution to our students, the local economy and to society in general.

The Editors

LABORATORY FOR NANOSTRUCTURED MATERIALS RESEARCH

Nicos C. Angastiniotis
Department of Mechanical Engineering, Higher Technical Institute, C. Kavafi Str., P.O.Box 20423, Aglantzia, 2152 Nicosia, Cyprus
e-mail: nangastiniotis@hti.ac.cy

BRIEF DESCRIPTION

The research strength of the Laboratory for Nanostructures Materials Research (LNMR) lies in nanostructural size control. It has the means and expertise to regulate the size of nanoparticle constituents from the amorphous to the nanocrystalline range; such capability enables the tailoring of local composition and consequently the making of nanoparticles with controlled physico-chemical properties. Specifically, the Laboratory possesses implementation rights of a patented process which focuses on the production of nanoparticles with amorphous based metallic constituents that yield dramatic changes in properties, due to confinement and compositional effects. Apart from its own nanoparticle manipulation capabilities the Laboratory has strong collaborative links with CRIF (RTD, Belgium), a nanoparticle manufacturer by atmospheric plasma torch, and the Fraunhofer-Institut für Keramische Technologien und Sinterwerkstoffe (RTD, Germany) which can provide dispersion and granulation capability. The Laboratory by agreement with KEAC Ltd in UK has also access to state-of-the-art fluidized bed technology.

RESEARCH ACTIVITY

The LNMR is in position to provide expertise in any of the following operating divisions:

Nanosynthetic capability

- To date nanosynthetic development tends to be irreproducible, producing nanoparticles with limited stability and uncontrolled crystallinity, i.e., non-uniform grain size, irregular structure, and variable composition with erratic or undesired stoichiometric or non-stoichiometric constituency.

- Our own metastability process has the enabling capability to convert each and every one of such particles into an integrated assembly of domains, each domain being as small as 1 nm, comprising therefore a near amorphous template or a collection of atomic or molecular clusters.

- Regulated low temperature, progressive, albeit quick and efficient, metastable, thermochemical treatment of such extraordinary nanoscale structure is shown to create stable and uniform building blocks with predefined grain size, structure, and tailor-made non-stoichiometric or stoichiometric composition.

- The premise of this approach is to arrest across predefined length scales that range from 1 to 100 nm, dramatic changes in properties, due to confinement and compositional effects.

- The metastability process constitutes a unique thermodynamic and kinetic tool that has the intrinsic advantage to operate with nanoscale precision, providing therefore, extraordinary nanosynthetic ability.

- The process had already been exemplified through the use of tungsten based prototype compositions (i.e., Co-WC, WC, WN, W-Cu, and W) and is currently applied on titanium, zirconium, silicon and aluminum based systems.

Predictive nanomaterial design

- The enabling capability of the metastability process to regulate the physico-chemical characteristics of particles should provide enhanced understanding of material properties across length scales which should sequentially lead to the ability to develop nanomaterials *via a priori* prediction of structure-property relationships.

- By using therefore the metastability process, a future database that details structure-property relationships at all length scales (1-100 nm) could be prepared.

- Conversely, such databases could be utilized as a reference for producing nanomaterial building blocks with predicted properties.

- Synthesis of these nanomaterials based on the predictive design rules should simply validate the understanding of fundamentals.

- These two approaches are inextricably intertwined and together will be needed in the future to provide the foundation for new nanosynthetic material production.

- By adopting this methodical, predictive approach we will be in position to identify and validate *a priori* structure-property-processing parameters.

- Such capability will enable the "bottom up" synthesis of nanomaterial building blocks with predictable properties.

Integrating nanomaterial building blocks into devices and products

- Predictive design comprises only the beginning in the progression from nanomaterials to dispersions and finally, to spatially resolved nanostructures.

- To realize the promise of predictive design, single and/or 3-D assemblies of building blocks must be incorporated into larger-scale devices and systems while retaining their novel attributes (the pertinent schematics are provided in Figures 1 and 2).

- Incorporating nanomaterial building blocks into thin films, coatings, and net-shaped components will require the design and development of processes that retain the properties and functionality of the nanoscale building blocks.

CURRENT PROJECTS

Nanosynthetic capability

Main deliverable: Create stable and uniform building blocks with predefined grain size, structure, and tailor-made stoichiometric or non-stoichiometric composition.

Impact: Dramatic changes in properties, due to confinement and compositional effects.

FP6-NMP Network of Excellence (KMM-NoE) 2005 – 2008

Predictive nanomaterial design

Main deliverable: A database that details structure-property relationships at all length scales (1-100 nm).

Impact: Development of nanomaterials via a priori prediction of structure-property relationships.

Industries: Powder producers.

In partnership with CRIF (Centre de Recherche des Industries Technologiques) at Liège Belgium

INTERREG IIIA / Greece – Cyprus 2006 – 2008

Manufacturing scale-up and processing

Pilot line to study, develop and scale-up nanotechnology-based processes from laboratory.

Integrating nanomaterial building blocks into devices and products

Main deliverable: Incorporate the predefined nanoscale functionality of the nanomaterial building blocks into thin films and coatings for targeted applications.

Impact: The ability to produce nanomaterial building blocks that deliver predefined functionality tailored to specific applications will be taking nanoscience and nanotechnology to the next level: safe, reproducible, cost-effective, deliberate, predictive design and fabrication capability to provide levels of functionality and performance not available nowadays.

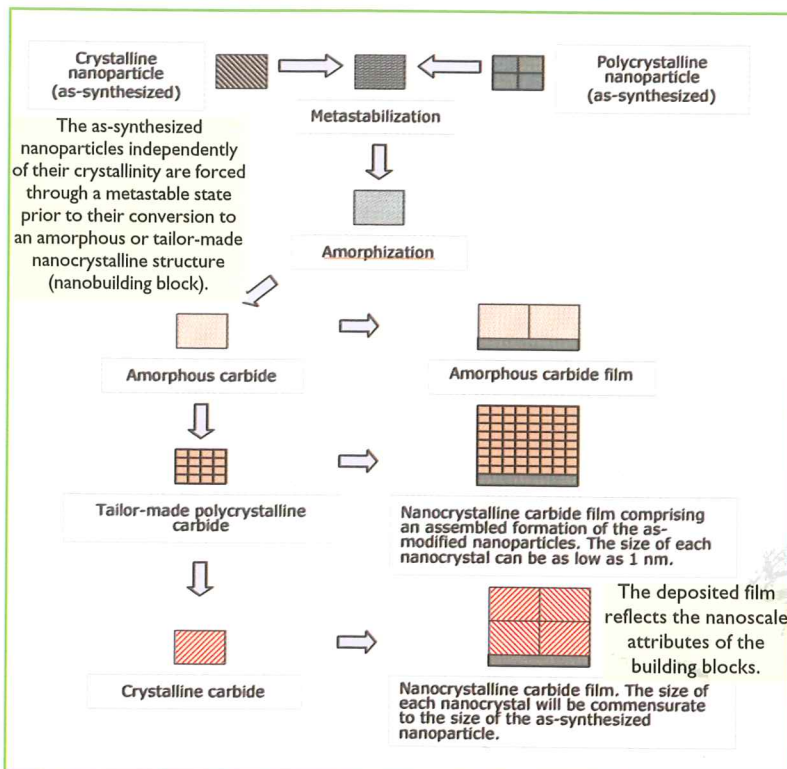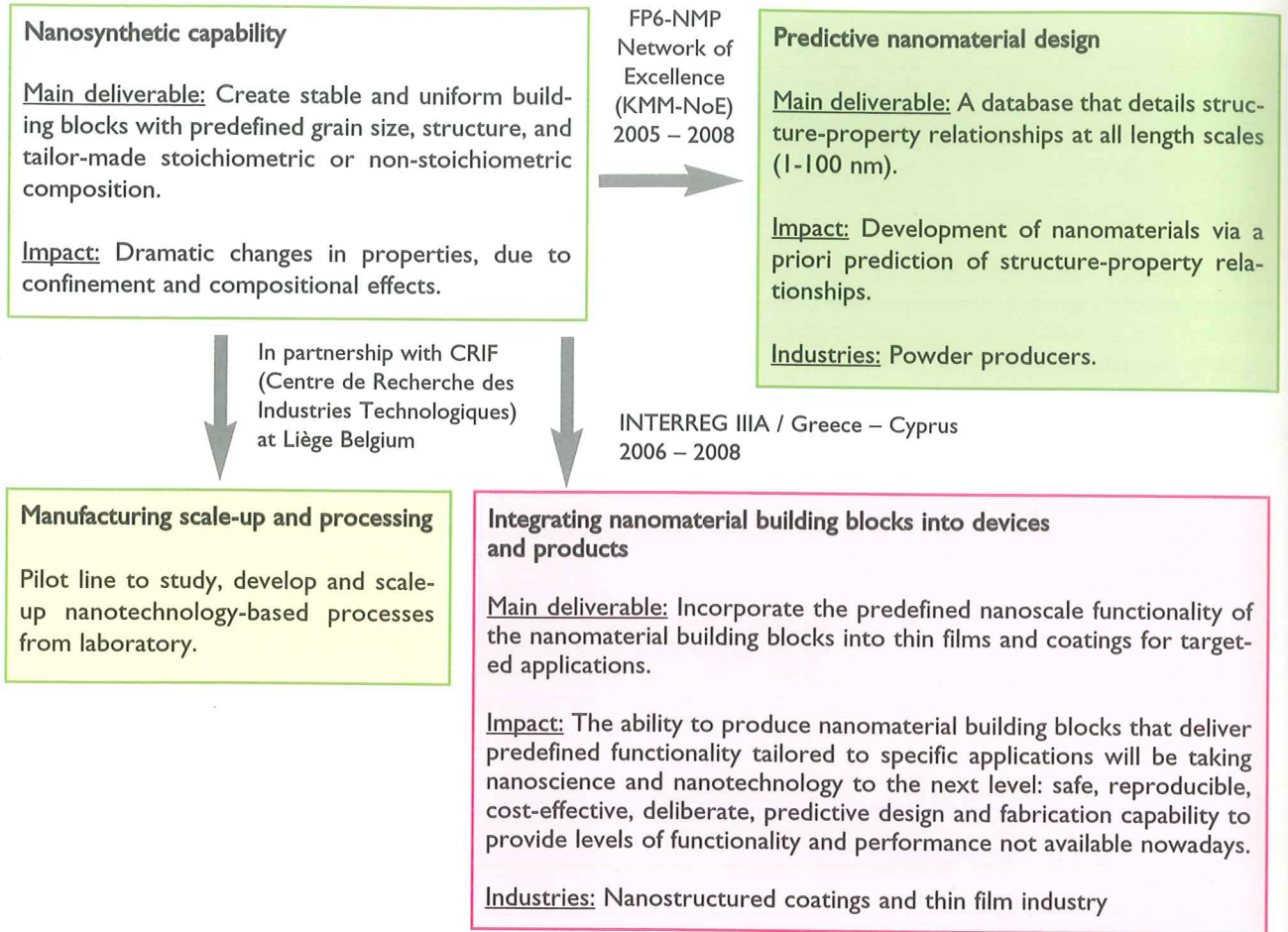Industries: Nanostructured coatings and thin film industry

Fig. 1. Transposing the nanoscale attributes of single building blocks into thin film functionality.
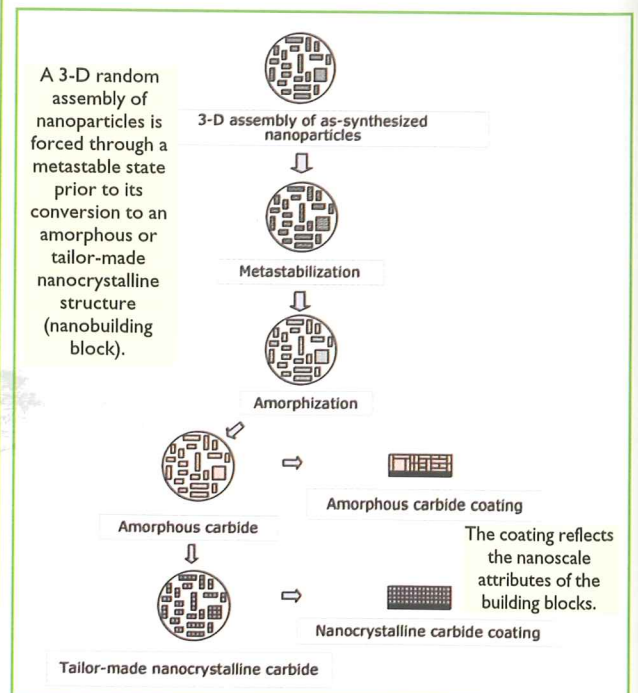

Fig.2. Transposing the nanoscale attributes of 3-D building block assemblies into coating functionality.

Measurement System Analysis & Capability Studies

Dr. Ioannis Angeli, Lecturer of Higher Technical Institute
Mr. Demetris Zangoulos, 6 Sigma Project Manager (Black Belt), CTC Plc

1.1 Introduction

Six Sigma is a management philosophy that helps organizations to become more effective and more efficient. The last two decades Six Sigma has evolved from a simple quality metric to an overall strategy that accelerates improvements and achieves impressive results of performance; always corresponded to the customer critical requirements. The Six Sigma approach aims to reduce defect levels to only a few parts a million for an organization's key products and processes. It accomplishes this level of performance by using a variety of managerial tools as well as the art of statistics. Statistical thinking is a philosophy of learning and action based on the principle that the reduction of variation is a key issue for success. Next, it will be explained how the process and the measurement system can be evaluated in a proper manner within the Six Sigma principles, in order to make right decisions and take corrective actions.

1.2 Variation

Any production process contains many sources of variation that deviations the organization's performance and reduce the quality level of products being produced and services being provided. If these sources of variation appears constantly and presented as a natural part of a process they referred as common causes of variation. On the other hand, there are some sources of variation that arise from external – unpredictable causes and they referred as special causes of variation. Although, common causes of variation can be predictable and through a valid analysis could be avoided the special causes of variation are unexpected and most of the times are out of control.

Furthermore, the total variation observed in a process can be described as the aggregation of the process variation produced both from common and special causes and the measurement system variation due to the inability of the measurement system to measure constantly. Prior the evaluation of the process variation, it should be first completed measurement system verification as shown on Figure 1.
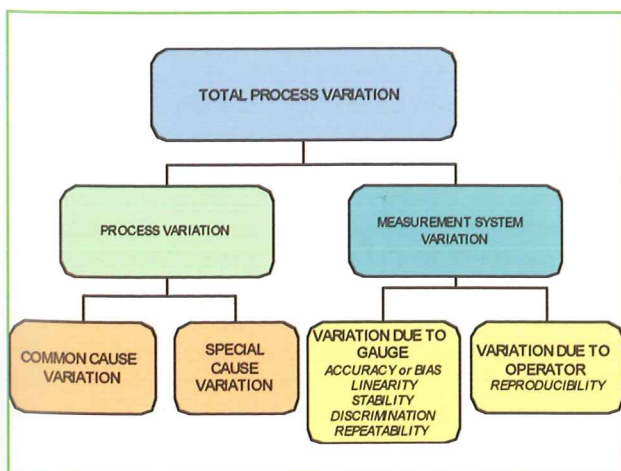

Figure 1: Total Process Variation

2.1 Measurement System Analysis

The evaluation of data obtained from inspection and measurement is meaningful only if the measurement system is accurate, precise, and reproducible. Otherwise, products that are not within specifications might reach to the customer or products that are within specifications might consider as defective. Therefore, by referring to figure 2, accurately assessing Six Sigma performance depends on reliable measurement systems. Measurement System as a concept is very complex involving factors such as people, devices, procedures, standards, and training.
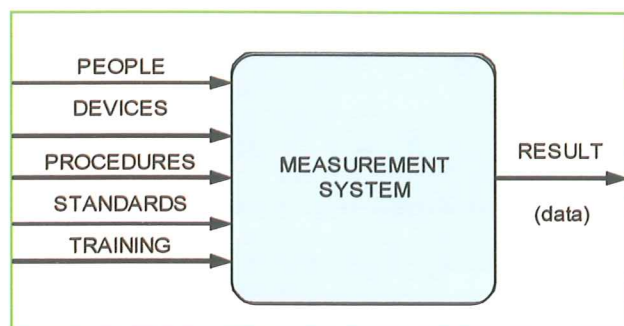

Figure 2: Measurement System Analysis

2.1.1 Reproducibility & Repeatability

When some one measures the same unit multiple times, the results will usually vary. The variation observed when the same person using the same instrument measures a part, is called equipment variation or repeatability. On the other hand, when an instrument is used by different individuals for measuring the same part the variation observed, is called operator variation or reproducibility. Both, equipment and operator variation can be successfully evaluated and quantified by using statistical approach. In particular, repeatability and reproducibility require a study of variation that can be addressed through statistical analysis. A repeatability and reproducibility study is conducted by following the procedure being described in the next subchapter.

2.1.2 Steps of Repeatability & Reproducibility Studies

The following methodology and steps should be followed to carry our Repeatability & Reproducibility Study:

1. Select m operators and n parts. Typically at least two operators and 10 parts are chosen. Number the parts, so that the numbers are not visible to the operators.
2. Before starting the measuring the measuring instrument should first calibrated with reference standards.
3. Let each operator measure each part in a random order and record the results. Repeat this procedure for a total of r trials (at least two trials must be used). Let M_{ijk} represent the kth measurement of operator i on part j.

4. Compute the average measurement for each operator:

$$\overline{x_i} = \left(\sum_j \sum_k M_{ijk}\right) / nr$$

The difference between the largest and smallest average between the largest and smallest average is:

$$\overline{x_D} = \max_i\left\{\overline{x_i}\right\} - \min_i\left\{\overline{x_i}\right\}$$

5. Compute the range for each part and each operator:

$$R_{ij} = \max_k\left\{M_{ijk}\right\} - \min_k\left\{M_{ijk}\right\}$$

These values show the variability of repeated measurements of the same part by the same operator. Next, compute the average range for each operator:

$$\overline{R_i} = \left(\sum_i R_{ij}\right) / n$$

The overall average range is then computed as

$$\overline{\overline{R}} = \left(\sum_i R_i\right) / m$$

6. Calculate a "control limit" on the individual ranges R_{ig}:

$$\text{Control Limit} = D_4 \overline{\overline{R}} ,$$

where D_4 is a constant depends on the sample size (number of trials, r).
Once these basic calculations are made, an analysis of repeatability and reproducibility can be performed. The equipment variation (EV) is computed as

$$EV = K_1 \overline{\overline{R}}$$

Reproducibility or operator (or appraisal) variation (AV) is computed as:

$$AV = \sqrt{\left(K_2 \overline{x_D}\right)^2 - \left(EV^2 / nr\right)}$$

The constants K1 and K2 depend on the number of trials and number operators, respectively.
An overall measure of repeatability and reproducibility (R&R) is given by

$$R \& R = \sqrt{\left(EV\right)^2 + \left(AV\right)^2}$$

Repeatability and Reproducibility are often expressed as a percentage of the tolerance of the quality characteristics

being measured. A percentage of 10% is considered as excellent while a percentage between 10% - 30% is considered acceptable. Anything over 30% is unacceptable, and a corrective action should be taken. The following *Example 1 next*, is showing the calculations as developed by Minitab software.
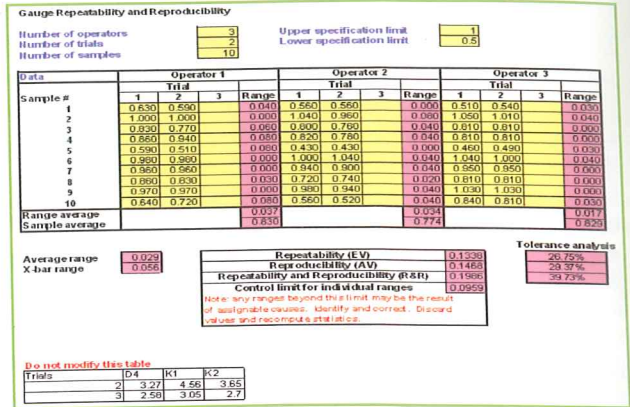
Example 1: Gauge Repeatability & Reproducibility (using Minitab)

Using the SPC Excel software witch is working within Microsoft Excel, a similar example with two operators, 5 samples, 3 trials each, is shown in example 2 .The graphs are presented too.
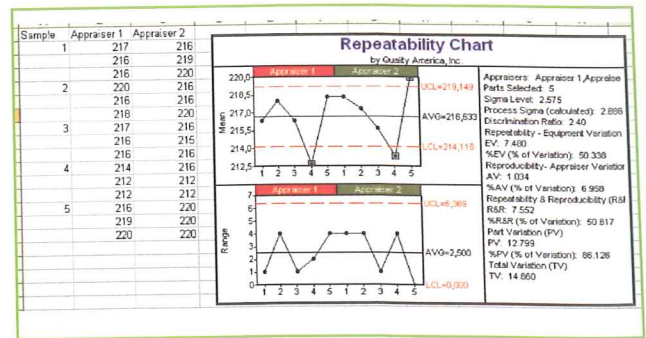
Example 2: Gauge Repeatability & Reproducibility (using SPC Excel V4)

2.1.3 Corrective Actions

Once the results have been obtained corrective actions should be then taken in order to improve both accuracy and precision of our measurement system. Accuracy is defined as the closeness of agreement between an observed value and an accepted reference value while precision is described as the closeness of agreement between randomly selected individual measurements or results. Equipment calibration is one of the most appropriate actions that could be taken in order to minimize measurement system variation. Calibration can be defined as the comparison of a measurement device or system having a known relationship to national standards against another device or system whose relationship to national standards is unknown. The usual recommendation is that equipment be calibrated against working level standards that are 10 times as accurate as the equipment. Furthermore, if the problem is due to operators' inability to reproduce same measurements the solution could be appraisals' training. Once the measurement system variation proved to be acceptable the process capability evaluation should be follow.

3.1 Process Capability

Process capability refers to a range of Key performance Indicators (KPI's) (metrics) that measure the ability of a process to deliver products or services within customer's requirements. In particular, process capability is the comparison of the VOP (Voice of the Process) to the VOC (Voice of the Customer). In Six Sigma methodology the process capability is measured by using the "Sigma Level" metric. There are two key advantages when using "Sigma Level" to measure process capability:

- It's a common capability measure that allows processes to be benchmarked against each other across different industries, technologies, data worlds etc.

- Their scale it's not linear. Sigma Levels have increasing resolution at low defect levels, allowing the difference between 99.8% and 99.9% (for example) to be reflected in a more significant way.

3.2 Process Capability Studies

At this subchapter it will be illustrated some of the most common process capability indices such as Cp and Cpk (in the short-term perspective) and Pp and Ppk (in the long-term perspective).

A process capability study is a carefully planned study designed to yield specific information about the performance of a process under specified operating conditions. Typical questions that are asked in a process capability study include the following:

- Where is the process centred?
- How much variability exists in the process?
- Is the performance relative to specifications acceptable?
- What proportion of output will be expected to meet specifications?

To be able to answer those questions, some process capability indices should be used. The capability study will be conducted after the process is under statistical control. This can be investigated by using the Statistical Process Control (SPC) control charts. If at least 20 samples inspected are within the Upper and the Lower Control Limits then you can proceed with capabilities studies.
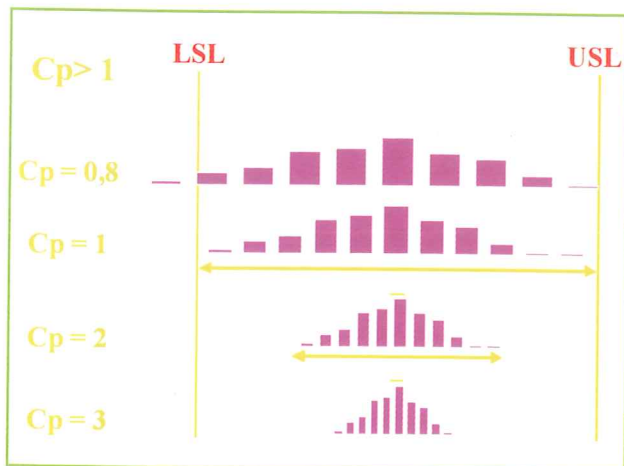
The C_p shown on figure 3, reflects the potential capability of the process without considering how centred the process is. Is comparing the spread with specifications:

$$C_p = \frac{VOICE\_OF\_THE\_CUSTOMER}{VOICE\_OF\_THE\_PROCESS} = \frac{Width\_of\_specification}{Width\_of\_histogram} = \frac{(USL - LSL)}{6 * \sigma_{st}}$$

The C_{pk} shown on figure 4, reflects the actual capability of the process by measuring the same ratio as the C_p, but only to the nearest specification limit, since this is the limit which is most likely to be failed. With other words is comparing the location of the process with respect to specifications:

$$C_{pk} = \frac{NEAREST\_VOICE\_OF\_THE\_CUSTOMER}{HALF\_OF\_VOICE\_OF\_THE\_PROCESS} = \frac{(NearestSpec - ProcessAverage)}{3 * Sigma}$$

The approach is exactly the same when calculating the potential as well as the actual process capability in the long term perspective; P_p & P_{pk}.

4. CONCLUSION

The performance of any process depends mainly from the total variation that is recorded at the implementation stage, with respect to time. Decreasing the variability with the use of charts of statistical control we can decrease the errors and increase at the same time the performance.

The right proceature for the development of a measurement system and analysis of data should pass from the following stages:

1. Select and specify the process that will be analyzed taking into consideration always their impact if anything goes wrong, to the enterprise and the customer.

2. Decide the method of measurement i.e., unit of measurement, sampling plan, frequency of sampling, operator, equipment needed, personnel training etc

3. Determination of the specifications for the particular product or service

4. Select or purchase the appropriate equipment with the right precision and accuracy

Figure 3: Graphical presentation of Potential Capability Cp
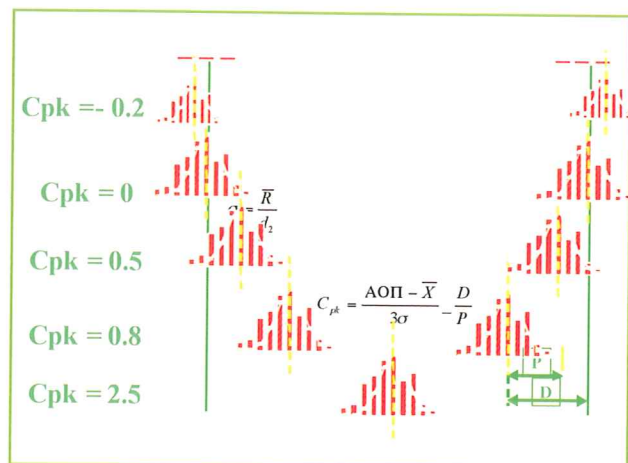
Figure 4. Graphical presentation of actual capability Cpk

11

5. Calibrate the equipment if needed

6. Run the reproducibility study of the equipment

7. Run the repeatability of operators

8. Commence production and sampling in accordance with a predefined sampling plan

9. After the collection of the first twenty samples and plotting them in the reselected SPC control chart, check the stability of the process (all the points inside the control limits)

10. Conduct the short-term capability study (calculate C_p and C_{pk})

11. If the process is under statistical control (all points within control limits) and the two indicators are above 1 (that is to say they are within specification), then the production can continued. If no, then with teamwork, corrective actions should be taken to bring the process under control and within specifications

12. Conduct of long-term capability study (calculate P_p and P_{pk})

13. Continue production targeting stabilisation and reduction of variation.

As a final conclusion it can be mentioned that is quit important to know the capability of the process and the process variation. It is also important to know the reliability of the measuring system and if is delivering accurate measurements. The combination of the above two will show up to what degree introversions are needed in order to improve the performance of the process under investigation.

GLOBAL WARMING AND THE HISTORY OF CARBON DIOXIDE THROUGH THE GEOLOGIC RECORD

Georgios Florides and Pavlos Christodoulides
Higher Technical Institute, PO Box 20423, Nicosia 2152, Cyprus

Abstract

Global warming is a fact established from actual measurements. What is causing it though, is not so clear and a lot of factors are blamed for it. The basic factors are changes in greenhouse gas concentrations and changes in the sun's intensity. Anthropogenic Carbon dioxide (CO2) increase has contributed to global warming in some part during the twentieth century, but Carbon dioxide increase is in part a result of the temperature rise and various natural processes, like ocean changes in CO2 solubility. Biological activity has generally benefited because of the CO2 increase. Palaeoclimatological data show that the content of carbon dioxide in the atmosphere in this geological aeon is at a minimum value. The history of CO_2 caused changes in the physiology of plants. At the beginning of their existence plants had no leaves, in another stage they produced leaves and captured CO_2 very effectively producing large deposits of coal and finally they changed their efficiency in photosynthesis to survive in a deficient environment. Solar radiation change shows good relation to the change of global temperature observed.

We do not really have a complete and total understanding of the functioning of earth's complex climate system and our scientific knowledge is not sufficient at present to give definite answers about the causes of global warming.

1. Introduction

Global warming is the observed increase in the average temperature of the Earth's near-surface air and oceans, experienced in recent decades. According to the Intergovernmental Panel on Climate Change (IPCC) of the United Nations, most of the observed increase in globally averaged temperatures since the mid-20th century is very likely due to the increase in anthropogenic greenhouse gas concentrations [1], which leads to the warming of the surface and lower atmosphere by increasing the greenhouse effect. This effect is the phenomenon at which water vapour, carbon dioxide, methane and other atmospheric gases absorb outgoing infrared radiation raising the temperature.

An increase in global temperature is feared to cause in turn other changes such as the rising of sea level and changes in the amount and pattern of precipitation. There may also be increases in the frequency and intensity of extreme weather events, changes in agricultural yields, glacier retreat, species extinctions, increases in the ranges of disease vectors and others.

2. The Facts

Meteorological stations record the temperature since 1850 on land and sea. All available data are combined and temperatures are expressed as anomalies from 1961-90, which is the period with the best coverage. The reason for this is to avoid problems resulting from the fact that stations on land are at different elevations, and different countries estimate average monthly temperatures using different methods and formulae. Data analysed with the above method are available to the public by the Climatic Research Unit datasets. The datasets have been developed in conjunction with Hadley Centre of the UK Met Office [2].

The mean global average temperature anomalies for each year for combined land and marine values are shown in Fig. 1. As it is observed there is definitely an increase of the mean global temperature since 1990 of about 0.6 °C.
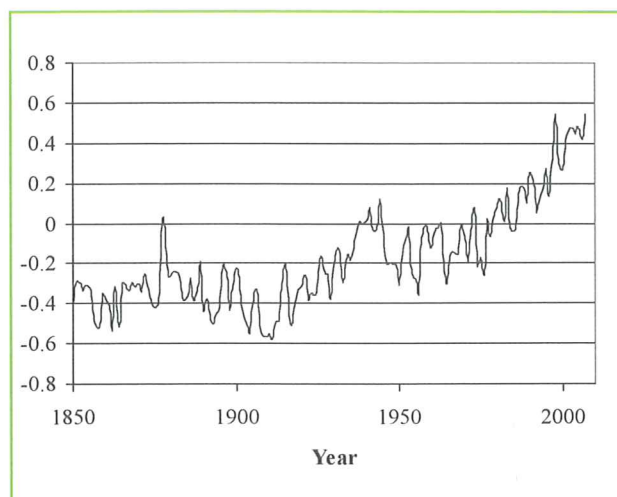
Fig. 1. Mean global average temperature anomalies for each year for combined land and marine values.

Scientists correlated the change in temperature with the known increase of greenhouse gases and especially carbon dioxide (CO_2) emissions, produced by the activities of mankind. CO_2 is the principal anthropogenic gas that is thought to affect the earth's radiative balance. It is a naturally occurring gas, and also a by-product of burning fossil fuels and biomass, it results also from land-use changes and other industrial processes. The correlation between the average temperature anomalies and the amount of CO_2 present in the atmosphere is presented in Fig. 2, where the variation of these quantities with time is plotted.

For this figure the global annual temperature anomalies, for the years 1856-2005 [3] are plotted together with the historical CO_2 record data from the Law Dome DE08, DE08-2, and DSS ice cores in Antarctica, for the years 1850-1978 [4], and the atmospheric CO_2 concentrations derived from air samples collected at the South Pole, for the period 1957-2004 [5]. The results show that although for both sets of data (those for temperature and CO_2 concentration) a rising trend is obvious for the last decades, there are large time intervals that the profiles do not follow the same trend, for example between 1900 to 1930.

Fig. 2. Temperature anomalies and historical CO2 record data showing some correlation between them.
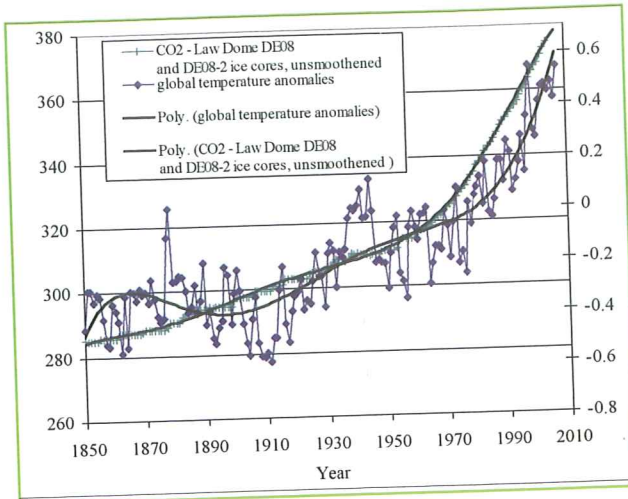
3. Further research in ice cores

During the past thirty years the Soviet Union drilled a number of holes at Vostok Station in Antarctica. The extracted ice cores produced a record of past environmental conditions stretching back to 420,000 years and covering four previous glacial periods.

Vostok Ice Core Data for 420,000 years [6] are shown in Fig 3. When researchers first looked at the results from these cores they observed a repeating correlation between CO_2 and temperature through the four glacial-interglacial cycles. But actually the timing of changes in this gas with respect to temperature is not accurately known because of uncertainty in the gas age and ice age difference. One way to overcome this inconvenience was to use records of atmospheric CO_2 content and temperature contained only in the trapped gases. Such an analysis was performed by Caillon et al., [7], for air bubbles in the Vostok core during Termination III (240,000 years before present). The sequence of events during Termination III suggests that the CO_2 increase lagged Antarctic deglacial warming by 800 ± 200 years and preceded the Northern Hemisphere de-glaciation. Thus there is an indication that CO_2 is not the forcing factor that initially drives the climatic system during a deglaciation and instead as the temperature increases, other factors are at work that cause the increase of CO_2 in the atmosphere.
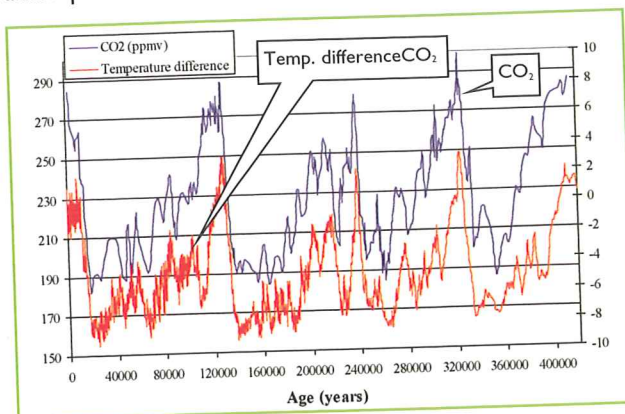

Fig 3. Vostok ice core data correlation between CO2 and temperature difference through the four glacial-interglacial cycles, for the last 420,000 years.

To have a better understanding of the data from the Vostock and Law Dome ice cores in Antarctica, the temperature difference was plotted against the CO_2 concentration as presented in Fig. 4. As it is shown, two different relations can be recognised, one for the Vostock data and a separate one for the Law Dome ice cores. The natural processes at work during the Vostock time period show that the concentration of CO_2 in the atmosphere increases with temperature. This happens in certain boundaries (shaded area in Fig. 4). The data from the Law Dome ice cores clearly show that the CO_2 concentration has by far exceeded these boundaries and that a certain increase in the temperature of the atmosphere may be due to this reason (with any reservation about the reliability of the published reference data). A temperature difference of about 2 degrees will be observed when the level of CO_2 concentration reaches 500 ppm, provided that all other factors do not change.
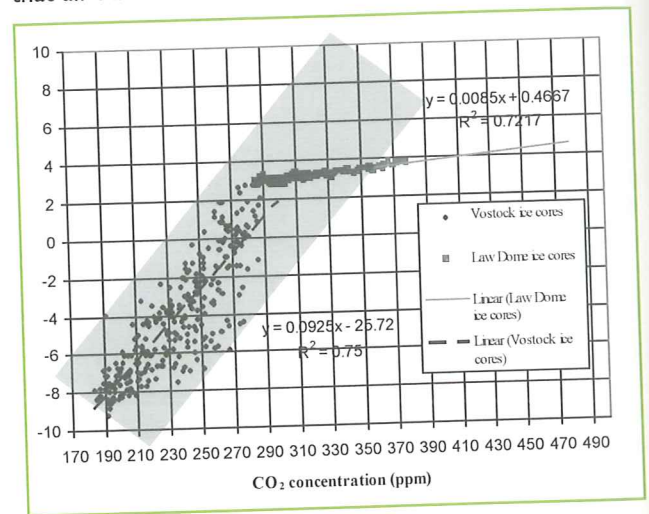
Fig 4. Vostok ice core data and historical CO2 record data from the Law Dome DE08, DE08-2, and DSS ice cores in Antarctica correlated to temperature difference.

4. The Geologic Record

Palaeo-climatologists calculated palaeolevels of atmospheric CO_2 using the GEOCARB III model [8]. GEOCARB III, models the carbon cycle on long time scales (million years resolution) considering a variety of factors that are thought to affect the CO_2 levels. The results are in general agreement with independent values calculated from the abundance of terrigenous sediments expressed as a mean value in 10 million year (Ma) time steps [9]. As shown in Fig. 5A during the early Palaeozoic CO_2 values were very high (about 15 times higher than at present), a large drop occurred during the Devonian (417-354 Ma) and Carboniferous (354-290 Ma), there were high values during the early Mesozoic (248-65 Ma) and a gradual decrease from about 170 Ma to low values during the Cainozoic (65 Ma to present).

In Fig. 5 B, C & D the range of global temperature through the last 500 million years is reconstructed. Fig. 5B, presents the intervals of glacial (dark colour) and cool climates (dashed lines). Fig. 5C, shows the estimated temperatures, drawn to time scale, from mapped data that can determine the past climate of the Earth [10]. These data include the distribution of ancient coals, desert deposits, tropical soils, salt deposits, glacial material, as

well as the distribution of plants and animals that are sensitive to climate, such as alligators, palm trees & mangrove swamps. Fig. 5D, presents the temperature deviations relative to today from δ18O records (solid line) and the temperature deviations corrected for pH (dashed line). It is clear that there is no statistical correlation between the level of carbon dioxide in the atmosphere and the temperature record through the last 500 million years. In fact, one of the highest levels of carbon dioxide concentration occurred during a major ice age that occurred about 450 million years ago.
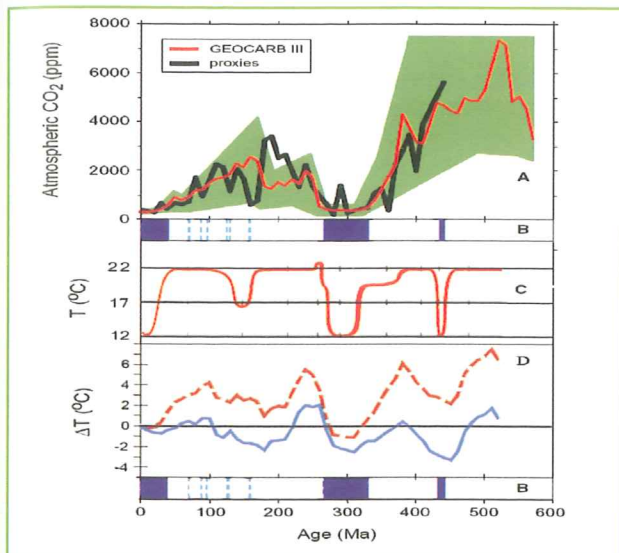

Fig. 5. A: GEOCARB III model results with range in error shown for comparison with combined atmospheric CO2 concentration record as determined from multiple proxies in average values in 10 Ma time-steps, redrawn from [9]. B: Intervals of glacial (dark colour) and cool climates (lighter colour) redrawn from [9]. C: Estimated temperature drawn to time scale. Data from Scotese, C.R., 2002 [10]. D: Temperature deviations relative to today (solid line) calculated by Shaviv and Veizer (2003) [11], from the "10/50" δ18O compilation presented in Veizer et al. (2000) [12]; Temperature deviations corrected for pH (dashed line) reconstructed by Royer et al., (2004) [9], redrawn from [13].

5. A closer examination of the Atmosphere of the Earth and the recorded role of Carbon Dioxide in geologic times

The atmosphere of the Earth consists mainly of about 78.08% nitrogen and 20.95% oxygen. The biggest minor component is the inert gas argon, making up 0.93%. Components at trace level include carbon dioxide (0.038%) the inert gases neon, helium and krypton, as well as hydrogen all well under 0.002%.

In addition, natural air always contains a certain amount of water vapour (0 - 7%). This is often neglected when giving the composition of air, although it is a very important constituent. The analogy of water vapour varies greatly with the air temperature, pressure, and humidity but typically makes up about 1% [14]. Carbon dioxide is the fifth largest component of the atmosphere but in reality is a minor constituent as mentioned above.

The geological records show that the great coal deposits of Earth were laid down mostly in the Carboniferous period (known as the first coal age) about 300 million

years ago. Coal formation continued throughout the Permian, Triassic, Jurassic, Cretaceous, and Tertiary Periods (known collectively as the second coal age).

Coal consists mostly of carbon, and this is how the Carboniferous was named. Coal is a member of a group of easily combustible, organic sedimentary rocks composed mostly of plant remains from ancient forests. As plants and trees died, their remains formed peat deposits in swamps that were buried by sediments from rivers and lakes. With deeper and deeper burial, the heat and pressure transformed the peat to coal.

A probable source of all this carbon was the atmosphere, presumably by conversion from gaseous hydrocarbons such as methane or possibly from free carbon dioxide. The massive deposits of high-carbon rocks laid down at the end of the Paleozoic (Fig. 6) therefore suggest a major change in the atmosphere at that time.

The World Energy Council, in a Survey of Energy Resources for Coal (including Lignite) [16], gives the recoverable reserves at the end of 1999 as 984,453 million tonnes.

Cretaceous at the end of the Mesozoic era (65 Ma) was another period of major change. Cretaceous comes from the Latin world 'creta' (chalk) because of the 'chalky' deposits of that period. Chalk largely consists of minute skeletons of single-celled algae and isolated plates of calcite derived from their breakdown together with the remains of other planktonic organisms. The chalk deposits accumulated at the shallower parts of the ocean floors between 500 – 4000 meters [17].

The carbonate mineral calcite is a chemical or biochemical calcium carbonate corresponding to the formula $CaCO3$ and is one of the most widely distributed minerals on the Earth's surface. Limestone is a sedimentary rock composed largely of this mineral, also formed during the Cretaceous period. Limestone often contains variable amounts of other material like silica, clay and silt in different forms within the rock. The primary source of the calcite in limestone is most commonly the shells of marine organisms especially corals and molluscs.

The role of atmospheric partial pressure of carbon dioxide (pCO_2) on marine organisms and ecosystems still remains poorly understood but again, a possible source of the Chalk and limestone could possibly be the conversion of the atmospheric carbon dioxide.
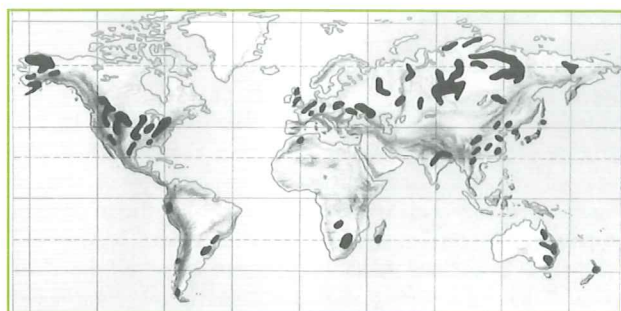

Fig. 6. Map showing the main carboniferous deposits of the world (redrawn from [15]).

The above changes were enormous and modified the atmosphere of the earth greatly. The relative amounts of carbon in different forms on earth are shown in Table 1 [17]. As it is observed the amount of carbon left in the atmosphere is actually extremely small. Almost everything that once was in the atmosphere has since been locked in the rocks.

Table 1. The major carbon reservoirs of the earth

Carbon reservoir	Kg $\times 10^{15}$
Carbon rocks (limestone, chalk, dolomite)	42000
Organic-rich rocks (oil, coal etc)	10500
Methane hydrates (including marine and continental deposits)	80
Oceans	38
Marine sediments	3
Soil and organic detritus	1.50
Atmosphere	0.76
Biosphere	0.56

Another point to consider is that there are three types of plants that differ in their efficiency of use of CO_2. These are called C3, C4, and CAM plants. It is thought that C3 plants (fixation of three molecules of CO_2 into a three-carbon sugar phosphate) are the ancestral form and evolved at a time of elevated CO_2 levels. Within the last 30 million years, in response to a period of low atmospheric CO_2 concentration and high O_2 concentration, following the Cretaceous period, C4 photosynthesis has evolved [18]. This is a more efficient method of photosynthesis in the lower CO_2 conditions. Modern plants have evolved to be carbon-dioxide 'hungry' and they have therefore produced mechanisms to chase after tiny amounts of it in the air.

Most plants are C3, including sugar beet, rice and potatoes; while maize and sugarcane are C4 plants. CAM (Crassulacean acid metabolism) plants are also plants with an extremely effective CO_2-concentrating mechanism and have adapted in arid environments and in environments in which the water supply is unpredictable.
Also, one more indication of the changing amount of carbon dioxide in the atmosphere comes from leaves. Leaves are the primary photosynthetic organs of most plants and are equipped with small openings or pores called stomata. These allow carbon dioxide to enter and oxygen to escape the leaf in order to facilitate photosynthesis. In addition, water is lost through stomata during a process called transpiration.

Simple leafless vascular plants first colonized the land in the Late Silurian - early Devonian period. These plants had few stomata, which served them well in a carbon dioxide rich atmosphere and helped them from drying out. 40 Ma after that period megaphyll leaves, Fig. 7, (leaves with a broad lamina (flat blade), like those of ferns and flowering plants) made their widespread appearance with their branched veins and planate form, at the close of the Devonian period at about 360 Ma ago. Beerling et al., [19] show that this delay was causally linked with a 90% drop in the atmospheric carbon dioxide concentration during the Late Palaeozoic era.
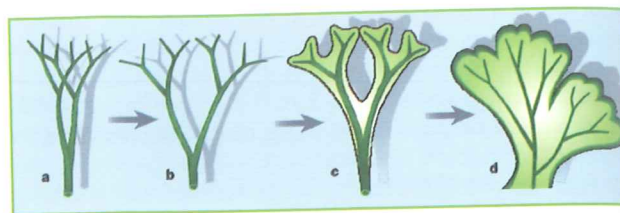

Fig. 7. Evidence for the evolution of megaphyll leaves with branched veins and a flat area for receiving sunlight, shows that they evolved from simple, leafless photosynthetic branching systems in early land plants (a, b) to dissected (c) and laminate (d) leaves over a period of at least 40 million years [19].

When planate leaves first appeared in the Late Devonian and subsequently diversified in the Carboniferous period, they possessed substantially higher stomatal densities. This observation is consistent with the effects of the pCO_2 on stomatal development Therefore, the drawdown in atmospheric pCO_2 in the Late Palaeozoic era and the concurrent observed increase in stomatal density, is a likely ancient example of plant response to lower concentrations of CO_2. Moreover, a 40-Myr delay between the axial form of Late Silurian/Early Devonian land plants and the development of megaphyll planate leaves is consistent with the timescale required to remove CO_2 from the atmospheric reservoir by silicate rock weathering and organic carbon burial.

From the above it is obvious that great changes have occurred in the atmosphere of the earth in the past aeons that affected life on earth and that the atmosphere could begin to acquire its present form in the Cenozoic aeon, after the death of the dinosaurs and the emergence of plants and animals that were relatives to those we know today.

Carbon dioxide could act as a fertilizer on biomass production because it is essential for plant nutrition and it has a positive effect on photosynthesis. Thus, biomass production could be higher following an increase in CO_2 concentration. Various field experiments, from numerous studies, demonstrate that plants exhibit positive gain when grown at elevated CO_2, although the magnitude varies greatly. Most crop responses range from 30 to 50 % increase in yield. Results from long-term experiments with woody species and ecosystems are even more variable. Huge growth responses (100 to nearly 300 % increase relative to controls) are reported from several tree experiments and the salt-marsh ecosystem experiment. Other results from experiments with woody species and the tundra ecosystem suggest little or no effect of CO_2 on physiology, growth or productivity [20].

In general, the strength of the response of photosynthesis to an increase in CO_2 concentration depends on the photosynthetic pathway used by the plant. Plants with the C3 photosynthetic pathway (all trees, nearly all plants of cold climates, and most agricultural crops including wheat and rice) generally show an increased rate of photosynthesis in response to increases in CO_2 concentration above the present level. Plants with the C4 photosynthetic pathway (tropical and many temperate grasses, some desert shrubs, and some crops including maize and sugar cane) already have a mechanism to concentrate CO_2 and therefore show either no direct photosynthetic response, or less response than C3 [21].

Carbon dioxide enrichment is commonly practiced in the cultivation of greenhouse crops because it increases both yield and profit. The response to this of pot plants, cut flowers, vegetables and forest plants is to increase dry weight, plant height, number of leaves and lateral branches. Also it is reported [22] that CO_2 enrichment increased the water-use efficiency by about 30%. Experiments on tomatoes have shown that CO_2, enrichment enhances fruit growth and colouring, and improves their ascorbic acid content. Furthermore, the elevated CO_2 results in higher sugar concentrations and related enzyme activities than in the control.

6. Human activities and greenhouse gas concentrations.

In this section the estimated human contribution to global warming is examined. Human activities contribute to the greenhouse gas concentrations through farming, manufacturing, power generation, transportation deforestation etc. Carbon dioxide is the most important anthropogenic greenhouse gas, mainly resulting from fossil fuel use. The global atmospheric concentration of carbon dioxide has increased as shown in Fig 2, from a pre-indus-

trial value of about 280 ppm to about 375 ppm in recent years. The atmospheric concentration of carbon dioxide now exceeds by far the natural range over the last 650,000 years (180 to 300 ppm) as determined from ice cores [1].

To demonstrate the effect that CO_2 has on climate the term Radiative forcing is used. Radiative forcing is a measure of the influence that a factor has in altering the balance of incoming and outgoing energy in the Earth-atmosphere system and is an index of the importance of the factor as a potential climate change mechanism. Positive forcing tends to warm the surface while negative forcing tends to cool it. Table 2 shows the Radiative forcing values for 2005 relative to pre-industrial conditions defined at 1750, expressed in watts per square metre (W/m2) [1]. The Radiative Forcing Value for carbon dioxide is 1.66 W/m2 and the total anthropogenic Radiative forcing is 1.6 W/m2.

Table 2. Global-average radiative forcing (RF) estimates and ranges in 2005 for anthropogenic elements and other important agents and mechanisms and the assessed level of scientific understanding. The net anthropogenic radiative forcing and its range are also shown [1].

RF Terms	Level of Scientific understanding	Radiative Forcing Values (W/m²)		
		Mean	Range	
			low	high
CO_2	High	1.66	1.49	1.83
CH_4	High	0.48	0.43	0.53
N_2O	High	0.16	0.14	0.18
Halocarbons	High	0.34	0.31	0.37
Stratospheric Ozone	Med.	-0.05	-0.15	0.05
Tropospheric Ozone	Med.	0.35	0.25	0.65
Stratospheric water vapour from CH4	Low	0.07	0.02	0.12
Land use	Med.-Low	-0.2	-0.4	0
Black Carbon on snow	Med.-Low	0.1	0	0.2
Total Aerosol Direct effect	Med.-Low	-0.5	-0.9	-0.1
Total Aerosol Cloud albeto effect	Low	-0.7	-1.8	-0.3
Linear contrails	Low	0.01	0.003	0.03
Total net anthropogenic		1.6	0.6	2.4
Solar irradiance	Low	0.12	0.06	0.3

7. Changes in ocean currents

Because of their huge masses, oceans should affect climate the most. The ocean absorbs much of the solar radiation reaching Earth. For visible light about 93% of a diffuse irradiance from above will be transmitted in the ocean [23]. In clear water, blue radiation may penetrate to considerable depths, whereas red radiation is mainly absorbed in the first few meters.

The rate of sensible heating of the oceans by the sun is slow because of the great heat capacity of the oceans. Even in the tropics, where the irradiance may be as high as 1000 W/m2, the heating is only 0.036 ГC per hour if all of this radiation is absorbed in the upper 10m. The cumulative effects of course are very large. In comparison, the amount of solar energy that is directly absorbed by the oceans is between 1.5 - 3 times as large as that absorbed directly by the entire atmosphere, and is more than three times as large as that absorbed by the entire global land surface [23].

The relation that exists between the solar irradiance and the sea surface temperature (SST) can be observed in Fig. 8.
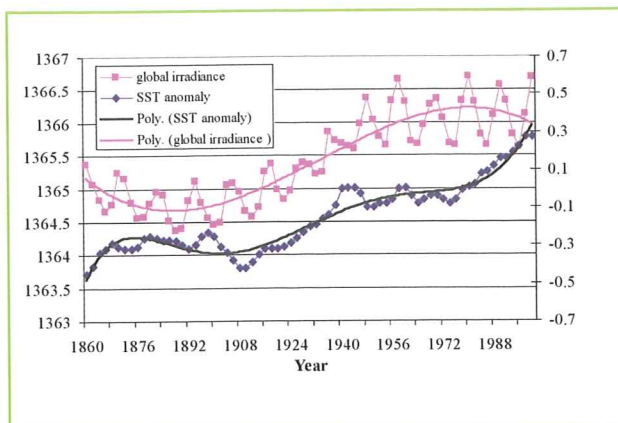

Fig. 8. Global solar irradiance [24] and smoothed annual sea surface temperature [25] indicating a good relation.

A relatively small fraction of this absorbed energy is transported over large horizontal distances by ocean currents. The largest part is stored locally or in the immediate vicinity and is later transmitted to the atmosphere mainly by evaporation and by long-wave radiation which drives atmospheric circulation. Water vapour condenses and forms rain. Condensation of water evaporated from warm seas provides the energy for hurricanes and cyclones.

Also, oceans play a significant role in distributing heat around the Earth, and therefore changes in ocean currents can bring about significant changes in climates from region to region. Temperature and salinity control the sinking of surface water to the deep oceans, which affects long-term climate change and drive a global circulation within the oceans sometimes called the Global Conveyor Belt.

Because of the Conveyor effect, warm surface waters, including the Gulf Stream, are propelled back into the North Atlantic. In winter, warm water transfers its heat to the frigid overlying air masses that come off from the ice-covered north. In this way warmed air masses make northern Europe climate milder in winter than comparable latitudes in North America.

Solar-induced warming and cooling periods ought to have produced significant changes in atmospheric CO_2 levels as well, as a result of ocean changes in carbon dioxide solubility. The accepted interpretation of the CO_2 increase does not consider this change to be a major source of atmospheric CO_2. The revelation that ancient temperature peaks coincided with increased atmospheric CO_2 levels following temperature change has not received the attention it deserves.

Concerning the CO_2 debate there is approximately 50 times more inorganic carbon in the global ocean than in the atmosphere. The solubility of carbon dioxide in the ocean increases in an inverse function with seawater temperature i.e. solubility is greater in cooler water and visa versa. One consequence of this is that when deep water up wells in warmer, equatorial latitudes, it strongly outgases carbon dioxide to the atmosphere because of the reduced solubility of the gas.

The balance of CO_2 concentration in the ocean is influenced also by a number of other processes. Phytoplankton for example, consisting mostly of algae and bacteria, are the foundation of the marine food chain. Drifting within the top surface layer of the ocean, it is thought to produce at least 40 percent of the food (i.e., organic carbon) made by photosynthesis on Earth each year. Phytoplankton plays a significant role in global climate. Since they use carbon dioxide for photosynthesis, they help keep atmospheric levels of the greenhouse gas in check. The larger the world's phytoplankton population, the more carbon dioxide gets pulled from the atmosphere and the lower the average temperatures on Earth [26].

The population of Phytoplankton depends greatly on the environmental temperature. There is evidence that during glacial periods, phytoplankton primary productivity increased, leading to an enhanced sedimentation of particulate organic carbon into the ocean interior [27].

8. Conclusions

The main conclusion drawn from this study is that solar radiation shows good relation to the change of temperature observed. Therefore it is logical to assume that this is the driving factor for the global warming.

Anthropogenic Carbon dioxide increase has contributed to global warming in some part during the twentieth century, but Carbon dioxide increase is in part a result of the temperature rise and various natural processes.

Biological activity has generally benefited because of the increase observed. Palaeoclimatological data show that the content of carbon in this epoch is at its minimum value. The history of CO_2 concentration in the atmosphere caused changes in plants. At the beginning of their evolution they had no leaves, in another stage they produced leaves and captured CO_2 very effectively producing large deposits of coal and finally they changed their efficiency in photosynthesis to survive in a deficient environment.

References

[1] INTERGOVERNMENTAL PANEL ON CLIMATE CHANGE, WMO, UNEP. Climate Change 2007: The Physical Science Basis, Summary for Policymakers. IPCC WGI Fourth Assessment Report.
< http://www.ipcc.ch/SPM2feb07.pdf>.

[2] Data from Hadley Centre of the UK Met Office. <http://www.cru.uea.ac.uk/cru/data/temperature/#dat dow>. See also: Rayner, N.A., P. Brohan, D.E. Parker, C.K. Folland, J.J. Kennedy, M. Vanicek, T. Ansell and S.F.B. Tett,: Improved analyses of changes and uncertainties in marine temperature measured in situ since the mid-nineteenth century: the HadSST2 dataset. Journal of Climate, 19 (2006), 446-469.

[3] Jones, P.D., D.E. Parker, T.J. Osborn, and K.R. Briffa. Global and hemispheric temperature anomalies--land and marine instrumental records, in Trends: A Compendium of Data on Global Change. Carbon Dioxide Information Analysis Center, Oak Ridge National Laboratory, U.S. Department of Energy, Oak Ridge, Tenn., U.S.A. Period of Record1856-2005, mean annual anomalies relative to the 1961-90 reference period (2006).
<http://cdiac.ornl.gov/trends/temp/jonescru/jones.html>.

[4] Etheridge, D.M., Steele, L.P., Langenfelds, R.L,. Francey, R.J., Barnola, J.-M. and Morgan, V.I.. Historical CO2 records from the Law Dome DE08, DE08-2, and DSS ice cores, in Trends: A Compendium of Data on Global Change. Carbon Dioxide Information Analysis Center, Oak Ridge National Laboratory, U.S. Department of Energy, Oak Ridge, Tenn., U.S. Period of Record 1832 A.D.-1978 A.D.CO2 (1998).
<http://cdiac.ornl.gov/trends/co2/lawdome.html>.

[5] Keeling, C.D. and T.P. Whorf. Atmospheric CO2 records from sites in the SIO air sampling network, in Trends: A Compendium of Data on Global Change. Carbon Dioxide Information Analysis Center, Oak Ridge National Laboratory, U.S. Department of Energy, Oak Ridge, Tenn., U.S.A. Atmospheric carbon dioxide record from the South Pole, record period 1957-2004, (2005).
< http://cdiac.ornl.gov/trends/co2/sio-spl.htm>.

[6] Petit, J.R., et al. Vostok Ice Core Data for 420,000 Years, IGBP PAGES/World Data Center for Paleoclimatology Data Contribution Series #2001-076. NOAA/NGDC Paleoclimatology Program, Boulder CO, USA. (2001).
<ftp://ftp.ncdc.noaa.gov/pub/data/paleo/icecore/antarctica/vostok/deutnat.txt> and
<ftp://ftp.ncdc.noaa.gov/pub/data/paleo/icecore/antarctica/vostok/co2nat.txt>

[7] N. Caillon, J. P. Severinghaus, J. Jouzel,JM Barnola,J Kang, V. Y. Lipenkov. Timing of Atmospheric CO2 and Antarctic Temperature Changes Across Termination III. (2003). Sience 299

[8] Berner, R.A. and Z. Kothavala. GEOCARB III: A Revised Model of Atmospheric CO2 over Phanerozoic Time, IGBP PAGES/World Data Center for Paleoclimatology, Data Contribution Series # 2002-051. NOAA/NGDC Paleoclimatology Program, Boulder CO, USA. (2001).
<http://www1.ncdc.noaa.gov/pub/data/paleo/climate_forcing/trace_gases/phanerozoic_co2.txt>

[9] D. L. Royer, R. A. Berner, I. P. Monta•ez, N. J. Tabor, D. J. Beerling, CO2 as a primary driver of Phanerozoic climate. (2004) GSA Today 14; no. 3, doi: 10.1130/1052-5173.
<http://www.soest.hawaii.edu/GG/FACULTY/POPP/Royer%20et%20al.%202004%20GSA%20Today.pdf>

[10] Scotese, C.R., PALEOMAP Project, Arlington, Texas. 2002 <http://www.scotese.com>.

[11] Shaviv, N.J., and Veizer, J. Celestial driver of Phanerozoic climate? (2003). GSA Today, 13, no. 7, 4–10.

[12] Veizer, J., Godderis, Y., and François, L.M., Evidence for decoupling of atmospheric CO2 and global climate during the Phanerozoic eon (2000). Nature,408, 698–701.

[13] Ridgwell, A. A Mid Mesozoic Revolution in the regulation of ocean
Chemistry. Revised for Marine Geology (2004).
<http://lgmacweb.env.uea.ac.uk/e114/publications/manuscript_phanerozoic_carbonate_cycling.pdf.>

[14] NASA' s Website:Earth's Atmosphere, <http://liftoff.msfc.nasa.gov/academy/space/atmosphere.html> and Earth Fact Sheet
<http://nssdc.gsfc.nasa.gov/planetary/factsheet/earthfact.html>

[15] Arduini, P. and Teruzzi, G.. Prehistoric Atlas. Blitz Editions an imprint of Bookmart Limited, Registered number 2372865, Leicester, UK. (1994). ISBN 1 85605 220 6.

[16] World Energy Council, Survey of Energy Resources, Coal (including Lignite).
<http://www.worldenergy.org/wec-geis/publications/reports/ser/coal/coal.asp>

[17] Skelton, P. W. The Cretacious World. The Open University, Cambridge, Cambridge University Press, (2003). ISBN 0521538432.

[18] Von Caemmerer S. (Susanna), Leegood, R. C., Sharkey T. D.. Photosynthesis: Physiology and Metabolism. Springer, (2000). ISBN 0792361431.

[19] Beerling, D. J., Osborne, C. P., Lomax, B. H. and Chaloner, W. G.. Biophysical constraints on the origin of leaves inferred from the fossil record. Nature (2001), 410. <www.nature.com>

[20] Dahlman, R.C. CO2 and plants - revisited. Vegetatio 104 (1993) 339-355.

[21] The Intergovernmental Panel on Climate Change (IPCC). The Carbon Cycle and Atmospheric Carbon Dioxide p 195. CLIMATE CHANGE 2001: THE SCIENTIFIC BASIS.
< http://www.grida.no/climate/ipcc_tar/wg1/index.htm>

[22] Islam, S., Matsui, T. and Yoshida, Y. Effect of carbon dioxide enrichment on physico-chemical and enzymatic changes in tomato fruits at various stages of maturity. Scientia Horticulturae 65 (1996) 137-149

[23] Kraus, E. B. Contributor Businger, J. A.. Atmosphere-Ocean Interaction. Oxford University Press US. (1994). ISBN 0195066189.

[24] Lean, J. Solar Irradiance Reconstruction. IGBP PAGES/World Data Center for Paleoclimatology Data Contribution Series # 2004-035. NOAA/NGDC Paleoclimatology Program, Boulder CO, USA.
<http://www1.ncdc.noaa.gov/pub/data/paleo/climate_forc ing/solar_variability/lean2000_irradiance.txt>

[25] Smoothed annual SST, 1861-2000, relative to 1961 to 1990, from USA National Climate Data Centre, Quayle et al. (1999). Redrawn from: The Intergovernmental Panel on Climate Change (IPCC). CLIMATE CHANGE 2001: THE SCIENTIFIC BASIS. < http://www.grida.no/climate/ipcc_tar/wg1/fig2-5.htm>

[26] NASA. Earth Observatory <http://earthobservatory.nasa.gov/Study/Polynyas/>

[27] Raven, J. A. and Falkowski, P. G. Oceanic sinks for atmospheric CO2 Plant. Cell & Environment 22 (1999) 6 741–755. doi:10.1046/j.1365-3040.1999.00419.x

DEVELOPMENT OF AN ELECTRICALLY TUNEABLE BRAGG GRATING FILTER IN POLYMER OPTICAL FIBRE OPERATING AT 1.55 µm

K Kalli[1], H L Dobb[2], D J Webb[2], K Carroll[2], C Themistos[3],
M Komodromos[3], G-D Peng[4], Q Fang[5] and I W Boyd[5]
[1] Nanophotonics Research Laboratory, Higher Technical Institute, C Kavafi Street, Nicosia 2152, Cyprus
[2] Photonics Research Group, Aston University, Birmingham B4 7ET, UK
[3] Frederick Institute of Technology, Cyprus
[4] University of New South Wales, NSW, Australia
[5] Department of Electrical Engineering, University College London, London, UK
E-mail: kkalli@hti.ac.cy

Abstract

We present a thorough study on the development of a polymer optical fibre-based tuneable filter utilising an intra-core Bragg grating that is electrically tuneable, operating at 1.55 µm. The Bragg grating is made tuneable using a thin-film resistive heater deposited on the surface of the fibre. The polymer fibre was coated via the photochemical deposition of a Pd/Cu metallic layer with the procedure induced by VUV radiation at room temperature. The resulting device, when wavelength tuned via Joule heating, underwent a wavelength shift of 2nm for a moderate input power of 160mW, a wavelength to input power coefficient of −13.4pm/mW and time constant of 1.7s⁻¹. A basic theoretical study verified that for this fibre type one can treat the device as a one dimensional system. The model was extended to include the effect of input electrical power changes on the refractive index of the fibre and subsequently to changes in the Bragg wavelength of the grating, showing excellent agreement with the experimental measurements.

Keywords: Optical fibre sensors, fibre Bragg gratings, polymer optical fibre, photosensitivity, wavelength tuning

1. Introduction

There are many important applications for tuneable fibre devices in optical measurement, sensing and lightwave communication systems, principally as reconfigurable and/or switchable real-time signal processors. In many cases all-fibre optical devices are the preferred choice as light can be manipulated in the optical fibre itself, with the tunability most often implemented via external means through piezoelectric, thermo-optic, or electro-optic effects [1–3]. Progress in the development of optical fibres in materials other than silica has made it desirable to examine the behaviour of these alternative tuneable devices. This paper provides a thorough study of the development of a polymer optical fibre-based tuneable filter utilising an intra-core Bragg grating that is electrically tuneable, operating at 1.55 µm.

The use of fibre Bragg gratings (FBG) as tuneable filters has been demonstrated in glass fibres with wavelength and bandwidth tunability brought about using strain [4] and temperature [5, 6]. FBG filters coated with thin film surface heaters have been promoted as wavelength tuneable devices because of their compact nature, fast response and high efficiency. There are numerous examples of re-configurable add/drop filters [7], tuneable loss filters [8, 9], and tuneable dispersion compensation [5,10]. The thin film surface heaters alter the local refractive index of the grating in a well-defined manner that is tuneable with input voltage [10]. The temperature gradient, which in turn defines the variation in the Bragg grating index modulation, is defined by the thickness of the film profile. Furthermore, the film thickness impacts the axial heat diffusion length, which when small can lead to the design of tailored heating profiles. Perhaps the greatest limitations to wavelength tunability are the thermal properties of the host glass fibre.

Polymer optical fibre (POF) Bragg gratings have high temperature sensitivity [11] and may be suitable candidates for producing a widely tuneable filter by heating the fibre. Thermally tuned gratings in polymer waveguides indicate large wavelength tuning, but in polymer materials that cannot be extruded into fibre [12]. The potential for all-organic optoelectronic circuits, with applications to data communications (filters, modulators, switches, and for data storage), sensing, detectors and LEDs, and organic lasers have spurred this interest. The benefits result principally from the manufacture of novel devices, in a chemically adaptable material, with low infrastructure costs compared with processing glass. Polymers may be tailored to specific applications, and dopants selectively incorporated into the structure.

Here we disclose the development of the first wavelength tuneable POF Bragg grating filtering device that relies on thin-film resistive load heating to produce wavelength changes. A discussion of the photo-reactivity of poly methyl methacrylate (PMMA), the host fibre material, is followed by an outline of the grating inscription procedure. A comparison through modelling of silica- and polymer-based fibre and fibre Bragg gratings is followed by the practical demonstration and characterisation of the filter.

2. Photo-reactivity in PMMA polymer-based optical waveguides

We present an overview of photo-reactivity in PMMA, which is relevant to the work in this paper. The principal refractive index increase, induced by laser irradiation at 325 nm in PMMA, results from a density increase in the laser-irradiated region, via photo-induced polymerisation of unreacted monomer.

The "photo-refractive effect" has been observed in several types of photopolymers, much effort has been directed to using PMMA as a base material for modification, as it is well characterised. From a commercial point of view PMMA ($C_5H_8O_2$), Teflon-AF (($C_4F_8O_2$)ₓ(C_2F_2)ᵧ), CYTOP-Asahi glass (C_6F_7O), and PFCB (F_6O_2+Aryl linkage) are amongst the most interesting polymers. However, as with all organic materials their performance at optical wavelengths is challenging as numerous strong absorption

bands dominate spectral features throughout the visible and near infrared. These are typically higher harmonics of C-H (for PMMA and PFCB), impairing their use at telecommunications wavelengths. Replacing these groups with C-F and C-O (as in CYTOP and Teflon-AF [13]) offers lower material losses at 1550nm, but has not been demonstrated in an optical fibre form. Issues of material loss can be offset by reduced Rayleigh scattering [14] as the polymer glass transition temperature is an order of magnitude less than silica. Waveguide applications demand that multiple copolymers are used from within the same compositional family limiting de-bonding, stress-optic influence and birefringence, whilst ensuring chemical, thermal, and mechanical compatibility.

2.1 Refractive index changes induced at 325nm

The photo-reactivity of PMMA-based material is not as apparent as for silica [15]. The foremost studies [16-19] were directed towards inducing grating structures and waveguides within slab polymers. Tomlinson et al. [16] reported that suitably prepared PMMA could exhibit a significant increase in refractive index when irradiated with a He-Cd laser (325nm). The essential step in the preparation of the samples was peroxidation of the monomer methyl methacrylate (MMA) in an oxygen-rich atmosphere prior to polymerisation. Several reaction pathways indicate [20, 21] a complex process that can include the polymeric peroxide (III) formed by copolymerisation of oxygen with MMA and methyl pyruvate, a photolysis product of the polymeric peroxide, which increases the UV absorption of MMA. Polymerisation can be initiated with a chemical initiator, typically azobisisobutyronitrile (AIBN) (50-200 mg/liter) at 40°C. Large refractive index increases reaching 3×10^{-3} have been reported with a resolution of at least 5000 lines/mm [16], and temperature increases are known to accelerate the index change but at the expense of the saturated value [19]. The presence of high concentrations of free radicals, created at low temperature, can lead to significant polymerisation. Therefore, the role of the peroxide is to act as a photo-initiator, sensitive to light at 325 nm. PMMA prepared from pure monomer using AIBN initiator only absorbs very weakly in this region and shows no photo-induced refractive index effect at 325 nm. Electron spin resonance has highlighted the difference of free radical concentrations in unirradiated and irradiated photo-reactive specimens [19]. The spectrum of the methacrylate propagating radical shows more than an order of magnitude increase in free radical concentration under UV irradiation. The refractive index increase accompanies an increase in material density [16], [18]. A proposition that the density increase is attributed to cross-linking through the monomer oxidation products [16], has failed to reveal the existence of any cross-linking by-products [18], and we conclude that cross-linking does not take place at all. Colburn and Haines have observed refractive index variations during volume hologram formation related to density differences [22], resulting from disparities in polymer concentration that developed during hologram formation. Evidence links the density increase in the UV-processing of PMMA with polymerisation of any residual monomer and the absolute value of the index change, with augmented polymer concentration in the UV-irradiated regions. Finally, the initial material density is inversely proportional to the refractive index increase, indicating

that weakly photo-reactive materials have higher initial densities than strongly photo-reactive samples. The rate of UV-induced polymerisation of MMA decreases markedly above 95% conversion, and polymerisation of the remaining monomer necessitates heating beyond the glass transition temperature (105-115°C) where again density increases occur.

What remains unclear is the exact role of UV-induced heating during focussed laser exposure. The generation of interference fringes, to produce a grating structure, results in points of high and low UV intensity, and an accompaniment of heat that may prove significant. Given the low working temperature of PMMA, excessive focussing can damage the polymer making it extremely lossy and any grating unusable. Moreover, one will want to minimise heating under grating inscription as the low thermal mass of the polymer will result in efficient heat transfer, to the regions where there is low UV intensity, this can result in slow erasure of the grating or a weak grating with reduced modulation depth. It should also be made clear that the primary effect in polymer inscribed gratings is not heat related; rather heating may contribute to the polymerisation or even lock in the UV-induced effects. This has been confirmed as the same thermally induced increases in density can be generated by annealing a sample that has not been prepared from peroxidised monomer; however the sample is insensitive to any photo-induced effects from the He-Cd laser.

The growth dynamics of Bragg gratings are often used to extract information on the photosensitivity mechanism [15], and parallel categories (Type I and Type II) have been used with POF Bragg gratings [23-25]. However, these are not distinct grating types, but relate to the fact that the core and cladding are photo-reactive under excessive UV-irradiation (unlike photosensitive glass fibres [15]); eventually leading to catastrophic fibre failure. Deductions regarding the physical properties of POF grating types cannot be made through their growth dynamics. However, accelerated decay measurements can usefully compare gratings inscribed in different polymer materials.

2.2 Refractive index changes induced at other wavelengths

UV pulsed excimer laser lithography of PMMA has also been investigated at 193 and 248nm, with two distinct reaction pathways [26]. 248nm irradiation produces total side chain scission and under high fluence produces main chain scission and hydrogen abstraction, whereas 193nm irradiation produces partial side chain scission and the production of free methanol radicals. The refractive index modification of PMMA can reach 0.01 at 248 nm for modest intensities of 17mJ/cm². However, these laser wavelengths are of little practical use as the penetration depth in PMMA is only $\sim 10 \mu m$, tens of microns short of the optical fibre core. Femtosecond laser modification of PMMA at a wavelength of 387 nm has produced permanent refractive index changes of 4×10^{-3}, offering the potential of gratings in polymer optical fibre [27]. Gas chromatography-mass spectrometry analysis of volatile fragments and molecular weight distribution monitoring (size exclusion chromatography) suggested direct backbone cleavage and monomer formation.

3. Step index POF

The PMMA-based POF used in this work was drawn from a preform fabricated following the procedure described in [28]; whereby using a higher temperature for the core polymerisation increased the fibre thermal stability and strength. The fibre manufacture followed a multiple-step process whereby a hollow polymer preform was filled with core monomer mixture of MMA, ethyl methacrylate (EMA) and benzyl methacrylate (BzMA) that was thermally polymerised in an oven over an incremental temperature excursion of 65°C to 85°C for three days, a temperature below the cladding's glass transition temperature (~100°C). Thereafter polymer optical fibres were drawn at 270°C from the preform. The fibres had an outer diameter of ~240μm and 12μm core diameter and the fibres were nominally single mode at the wavelength of operation.

4. FBG inscription

FBG inscription in POF has been documented using both the phase mask technique [11] and a ring interferometer arrangement [29], with grating inscription undertaken using continuous wave or pulsed laser sources operating in either the 325nm [11] or 355nm wavelengths [29]. Very strong polymer fibre Bragg gratings with 28-dB transmission rejection and a line width less than 0.5 nm have been achieved [30]. In this work FBGs were inscribed into step-index single- and few-moded POF using the inscription arrangement of Figure 1, undertaken with a continuous wave, 30-mW Kimmon IK series HeCd laser emitting light at 325 nm. The inscription process was based on the standard phase mask technique. The phase mask had a pitch of 1060.85 nm, and was designed to produce a FBG at 1568nm in the POF, in contrast to the 1536 nm design wavelength for silica fibre. For successful fibre Bragg grating fabrication in polymer optical fibre, the fibre must be supported along its entire length in order to minimize the effects of air currents and laser-induced heating on the fibre position. Consequently, the fibre was rested on three v-grooves mounted on three-axis translation stages. The fabrication technique as a general approach has been published by others [11]. Our modified ver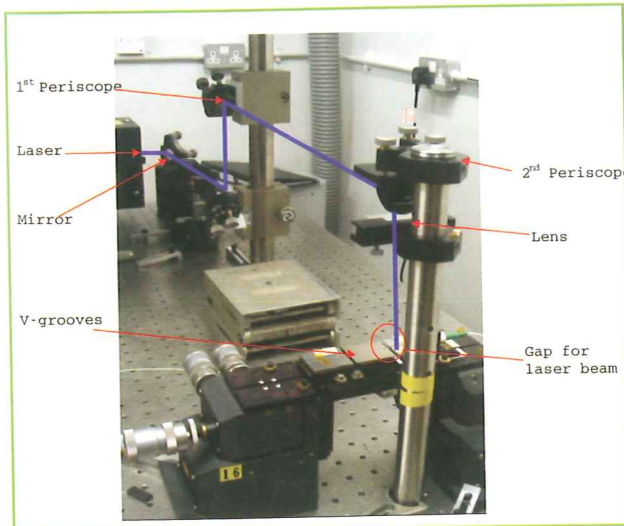tical-beam inscription set-up has extremely high yield and is particularly suited to use with POF (which is not as robust as silica fibre), unlike the more conventional horizontal-beam inscription phase mask approach. Two plano-convex cylindrical lenses with 10 cm focal lengths were incorporated in the system, one before the phase mask, which served to focus the light down into the core, and a second lens that was used to expand the 1 mm diameter laser beam to cover approximately 1 cm of the POF. Without the second lens incorporated in the arrangement, FBGs of approximately 1 mm in length, the size of the laser beam, could be fabricated. Thus, the second lens provided some flexibility over the grating design. Figure 2 shows a typical reflection spectrum for a grating, and we estimate that the reflectivity is approximately 10%, with a Bragg wavelength centred at 1579nm and 1nm bandwidth. Recent efforts have resulted in gratings as strong as 95% reflectivity, using the same inscription procedure. The low grating reflectivity may be attributed to the phase mask being designed for use at 248nm, not the 325nm inscription wavelength; therefore there is a small but significant zeroth order component that is incident on the POF during grating inscription, which adversely affects the inscription fringe contrast. The FBG inscription set up was tested by inscribing gratings into specially prepared silica fibre that is photosensitive to 325-nm laser light; exposure times exceeding two hours confirmed the stability of the inscription system to vibrations. In Figure 3 the Bragg grating inscribed into the POF is observed using a x100 oil immersion lens and microscope. Note from the figure that the FBG period can appear twice as large as the anticipated period of 530.4nm; a result of the formation of Talbot planes due to the imperfect suppression of the phase mask zero order [31]. The limited optical resolution of the microscope precludes the clear observation of fringes with the grating period.
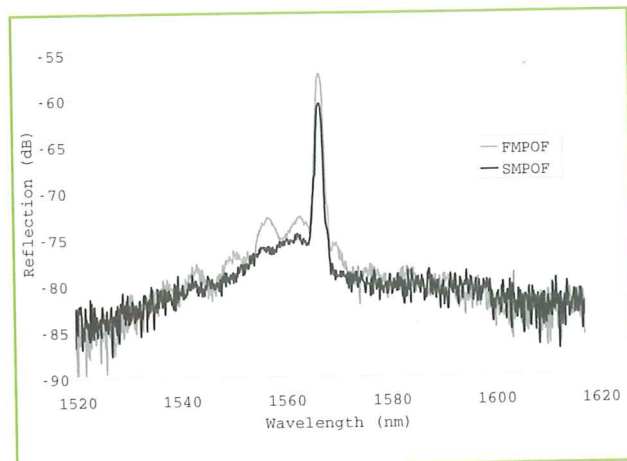
Figure 2. FBGs in few and single-mode POF OSA resolution 1 nm, length 10 mm.
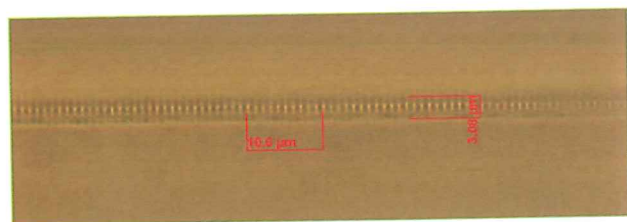

Figure 3. FBG in POF viewed with a 100x oil immersion DIC optical phase contrasting microscope. The grating period is measured as 1.06 μm a result of the formation of Talbot planes due to the imperfect suppression of the phase mask zero order.

Figure 1. Vertical set-up for FBG inscription. In this arrangement, the phase mask is placed on top of the V-grooves.

5. Modelling of silica- and polymer-based fibre Bragg gratings

In this section we investigate the design parameters of silica- and polymer-based FBGs using the full-vector magnetic (H) field formulation of the finite element method (FEM) [32] in conjunction with the coupled mode theory and the matrix transfer method [15]. The characteristics of the silica (SiO_2) optical fibres (SOF) and PMMA-based POF were explored to obtain the optimum properties for the design of the FBGs. The material dispersion characteristics are examined using the Sellmeier equations [33] and are shown in Figure 4, the refractive index for both the materials decrease with the wavelength, as expected.
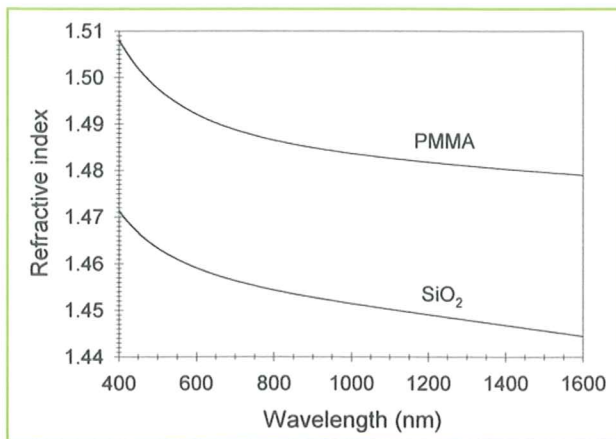

Figure 4. Material dispersion characteristics for SiO_2 and PMMA-based polymers.

The effective index variation with core diameter for SOF was calculated using the FEM. A standard silica-based optical fibre with a core and cladding index refractive indices of 1.447 and 1.444, respectively, at an operating wavelength of 1.55 μm was considered. The characteristics for the H_y magnetic field modes, shown in Figure 5, indicate that the effective index increases with the core diameter for both the fundamental and the first order modes. SOF exhibits single mode behaviour for a core diameter below 13 μm and no other higher modes are detected for the core diameter range examined. Similar calculations for the corresponding H_x modes indicate polarization independence.
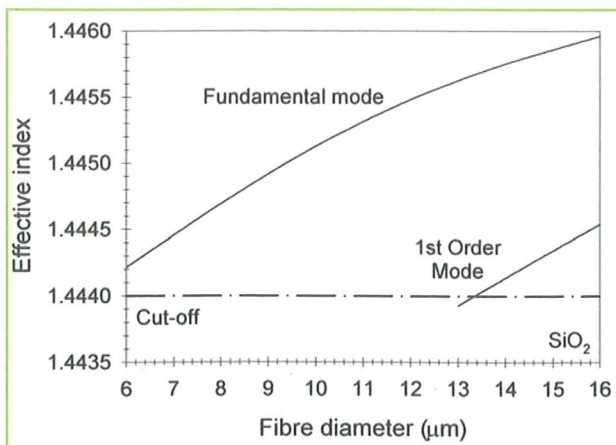

Figure 5. Effective index variation with core diameter for silica-based optical fibre.

Similarly, the effective index variation with core diameter is presented for PMMA-based POF, Figure 6. The refractive index for the PMMA material, from the Sellmeier equations [33], is 1.479372 at 1.55 μm, with an index contrast of 0.0086. It is interesting to note that with the greater confinement in the POF there are another two higher order modes present within the fibre diameter range examined, as shown in Figure 7, in addition to the fundamental and the 1st order mode. The first, second and third higher order modes exhibit respective cut-offs at fibre core diameters of 7.5 μm, 12 μm and 13 μm.
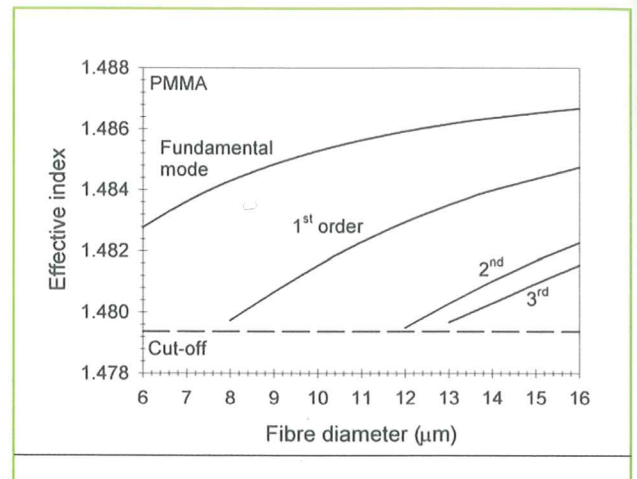

Figure 6. Effective index variation with core diameter for PMMA-based optical fibre.

Further, the effective field diameter (half power mode width) of the fundamental mode, with the variation of the fibre diameter of SOF and POF, has been calculated, Figure 8. The SOF has a higher effective field diameter indicating that the mode is less confined to the SOF core. Finally the field confinement factor (percentage of the field intensity present in the fibre core) of the fundamental mode with the variation fibre core diameter has been examined, Figure 9. The field has greater confinement in the POF core compared with SOF. The confinement factor of an optical fibre is proportional to the coupling coefficient used in a FBG and affects the power intensity spectrum of the device.

We conclude that since SOF has a lower refractive index compared with POF larger diameters can be used to ensure single mode operation. However, for a particular core diameter in POF the field has greater confinement, which will impact the FBG. Therefore, one anticipates greater FBG reflectivity in POF compared with SiO_2 for a given grating length.

The reflected power spectrum of SOF- and POF-based FBGs are investigated using the coupled mode theory (CMT) [34] and the transfer matrix method (TMM) [35]. The CMT is a very popular approach used in the analysis of optical fibres where the refractive index is weakly perturbed along the direction of propagation (z), such as in an FBG [36]. A fibre with such z-dependent non-uniformities cannot support individual modes of the unperturbed fibre. Nevertheless, in the ideal-mode approximation of the CMT, the fields of a perturbed fibre at a position z along the fibre can be described as superposition of the complete set of the bound and radiation modes of the unperturbed fibre. The transverse components of the
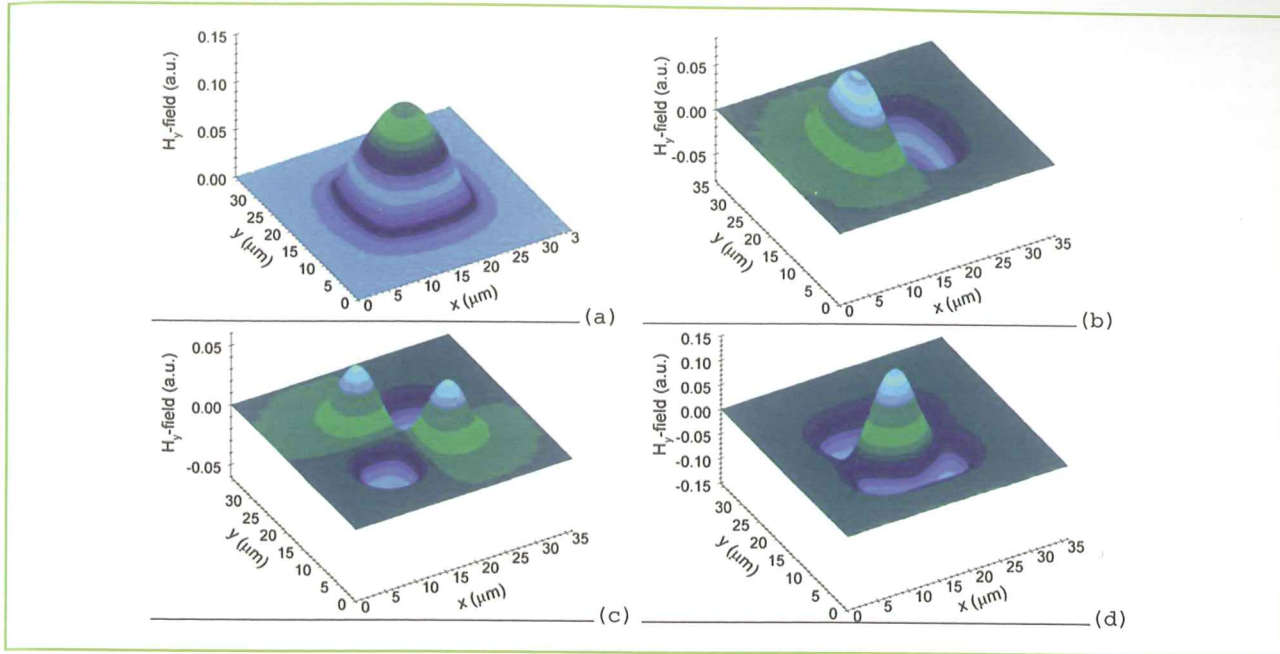
Figure 7. H_y field intensity of (a) the fundamental, (b) first-order, (c) second-order and (d) third-order propagating modes for a 16 μm PMMA fibre core diameter.
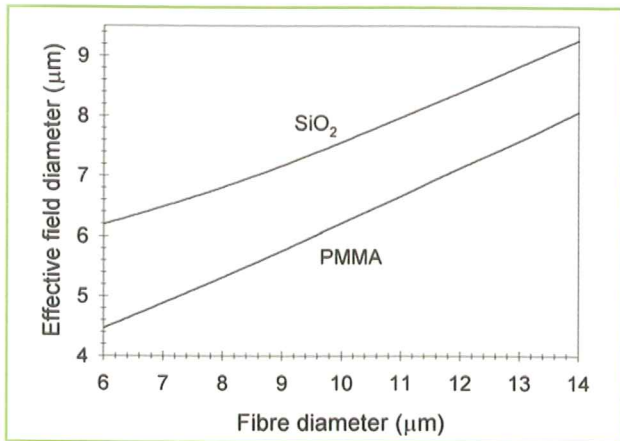
Figure 8. Effective field diameter for SOF and POF with the variation of the fibre core diameter.
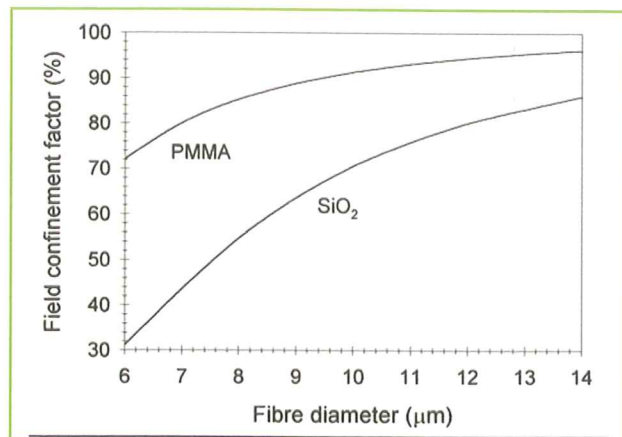
Figure 9. Optical confinement factor SOF and POF with the variation of the fibre core diameter.

electric and magnetic field can then be expressed as:

$$\vec{E}_t(x,y,z,t) = \sum_j \left[A_j(z)\exp(i\beta_j z) + B_j(z)\exp(-i\beta_j z) \right] \cdot \vec{e}_{jt}(x,y)\exp(-i\omega t) \tag{1}$$

$$\vec{H}_t(x,y,z,t) = \sum_j \left[A_j(z)\exp(i\beta_j z) - B_j(z)\exp(-i\beta_j z) \right] \cdot \vec{h}_{jt}(x,y)\exp(-i\omega t) \tag{2}$$

where $A_j(z)$ and $B_j(z)$ are the slowing varying amplitudes of the forward- and backward-propagating jth mode, respectively. $e_{jt}(x,y)$ ang $h_{jt}(x,y)$ are the transverse electric and magnetic mode fields, respectively. Although the modes in an unperturbed fibre are orthogonal and hence, do not exchange energy, the presence of dielectric perturbation causes the modes to be coupled and the evolution of the amplitudes $A_j(z)$ and $B_j(z)$ of the jth mode, along the fibre, can be described by a set of coupled ordinary differential equations as:

$$\frac{dA_j}{dz} = i\sum_k A_k(K_{kj}^t + K_{kj}^z)\exp\left[i(\beta_k - \beta_j)z\right] + i\sum_k B_k(K_{kj}^t - K_{kj}^z)\exp\left[-i(\beta_k + \beta_j)z\right] \tag{3}$$

$$\frac{dB_j}{dz} = -i\sum_k A_k(K_{kj}^t - K_{kj}^z)\exp\left[i(\beta_k + \beta_j)z\right] + i\sum_k B_k(K_{kj}^t + K_{kj}^z)\exp\left[-i(\beta_k - \beta_j)z\right] \tag{4}$$

where K_{kj}^t and K_{kj}^z are the transverse and longitudinal coupling coefficients between the modes k and j, respectively. In the transfer matrix approach the coupled mode equations (3) and (4) for a uniform fibre section, k, can be expressed in matrix form as:

$$\begin{bmatrix} A_k \\ B_k \end{bmatrix} = T_k \begin{bmatrix} A_{k-1} \\ B_{k-1} \end{bmatrix} \tag{5}$$

where A_k, B_k and A_{k-1}, B_{k-1} are the field amplitudes of the counter-propagating modes of the section, k and k-1, respectively. T_k is the transfer matrix describing the propagation through the uniform section and it is related to the coupling coefficients of the section. The approach can then be extended for all the uniform sections of the FBG as:

$$\begin{bmatrix} A_M \\ B_M \end{bmatrix} = T_M T_{M-1} ... T_1 T_0 \begin{bmatrix} A_0 \\ B_0 \end{bmatrix} \tag{6}$$

The peak reflected power of SOF- and POF-based FBG has been compared for two different device lengths, Figure 10. The peak reflected power increases with the fibre core diameter, and the POF-based FBG exhibits higher reflection than its SOF counterpart, as expected from the greater field confinement factor. As the device length increases the peak reflected power approaches 100% reflection.

The FBG filter stop-band with fibre core diameter is presented in Figure 11. As usual longer devices (5mm) exhibit a narrower stop-band for both the material systems. As the fibre core diameter increases the stop-band tends to increase slightly for all the cases examined, but the silica-based systems have narrower stop-bands than the POF

FBG. This results from the fact that for the POF-based FBG the Bragg condition is matched for a greater number of wavelengths, which again can be associated with the greater field confinement factor.

The increase of fibre length and core diameter increases the reflected power of both material systems, but respectively narrowing and widening of the stop-band. In all the cases examined POF-based devices exhibit a higher reflection spectrum and wider stop-band.

6. Metallic coating development and basic 1-D theory

In order to realise a practical, electrically tuneable device demonstration the POF FBG was coated with a palladium/copper metallic layer, the former of which aided adhesion to the PMMA surface and the latter acted as the thin-film heater element. Metal deposition was initiated using a vacuum UV (VUV) light source operating at 172 nm, at low (room) temperature and in a low vacuum of 10^{-2} mbar, with exposure times from 1 to 10 minutes [37]. At this wavelength the penetration depth of the light source is on the order of a micron and there is no damage to the grating, but the fibre surface is chemically roughened and the polymer bonds both physically and chemically to metallic particles.

The response of thin film heated Bragg gratings in POF is described with a differential equation giving the temperature distribution and thermal flow in the fibre, assuming both that the coating is uniform and of greater length than the grating giving a uniform temperature distribution, so only the radial distribution and thermal flow along the grating length are of importance. The device is modelled as a polymer cylinder with a thin-film thermal source on the surface enclosed by air. In this way the heat diffuses into the fibre core and the surrounding air, in addition to radiation. From energy conservation within the fibre [38],

$$\frac{\partial T(x,t)}{\partial t} = \kappa \frac{\partial^2 T(x,t)}{\partial x^2} + \frac{P_{in}(x,t) - P_{out}(x,t)}{\rho c_p \pi R_{fibre}^2} \tag{7}$$

where x is the distance along the fibre, $T(x,t)$ is the fibre temperature, κ, ρ and c_p are the thermal diffusivity, density and constant pressure heat capacity of the PMMA, R_{fibre} is the fibre radius. The thermal diffusivity κ is given by $K/(\rho c_p)$, where K is the thermal conductivity. $P_{in}(x,t)$ is the heating generated by the thin film heater, and $P_{out}(x,t)$ is the rate of heat loss from the fibre to the air. This is the most general form accounting for any non-uniformity in the coating and hence input power. Therefore, $P_{in}(x,t)$ = $I^2(t)R(x)$, where $R(x)$ is the local resistance per unit length of the coating and $I(t)$ is the electrical current. The heat loss from the metal to the air actually follows radiative heat transfer from two grey bodies of the form

$$\propto 2\pi R_{fibre} \sigma \left(T(x,t)^4 - T_{air}^4 \right) \tag{8}$$

where σ is the coefficient of thermal radiation dissipation. The low temperature range approximates this to $\propto (T(x,t) - T_{air})$. Given that the rate of heat loss is linearly proportional to the change in temperature we can write [37, 38],

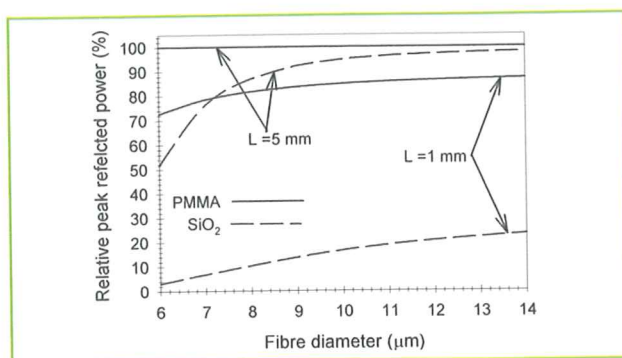$$P_{out}(x,t) = 2\pi R_{fibre} h T(x,t) \tag{9}$$

Figure 10. Relative reflected power with fibre core diameter, for SOF- and POF-based FBGs. Grating lengths of 1 and 5 mm are examined.

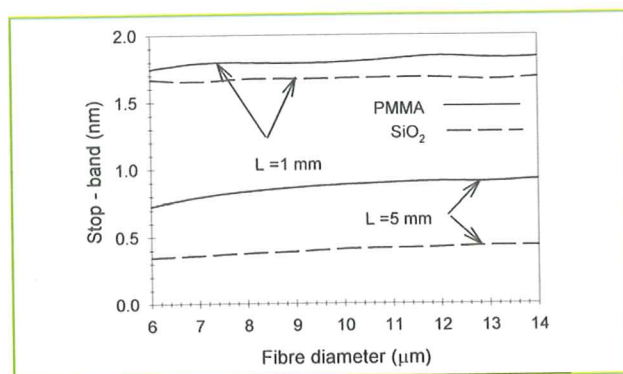Figure 11. FBG Stop-band with fibre core diameter for silica and PMMA FBG at a grating length of 1 and 5 mm.

where h is the surface conductance of the fibre, which characterizes the heat flow out of the fibre; additionally we introduce the constant a, which represents a lumped heat transfer coefficient due to heat transfer from the surface of the device,

$$\frac{P_{out}(x,t)}{\rho c_p \pi R_{fibre}^2} = aT(x,t) \qquad (10)$$

hence a is related to h by

$$a = \frac{2h}{\rho c_p R_{fibre}} \qquad (11)$$

Furthermore, radial heat flow terms have to be considered [37, 38],

$$2\pi R_{fibre} \kappa \frac{\partial T}{\partial r}\bigg|_{r=Rfibre} \quad \text{and} \quad 2\pi R_{fibre} \kappa_{air} \frac{\partial T_{air}}{\partial r}\bigg|_{r=Rfibre} \qquad (12)$$

where κ_{air} and T_{air} are the thermal diffusivity of air and the air temperature, respectively. This term is important as it accounts for temperature gradients that may exist *radially* across the grating. Given that the thermal conductivity of PMMA (0.17W/mK) is only 7 times that of air (0.025W/mK), compared with 55 times for silica glass (1.38W/mK) one should consider the validity of ignoring radial gradients and consider only heat flow along the length of the fibre. The heat flow through and along the surface of the fibre is characterized by the Biot number, $Bi = h\,R_{fibre}/K$. If the Biot number is sufficiently small (<0.1), meaning that the thermal conductance over the length R_{fibre} is far greater than the surface conductance then radial thermal gradients become negligible. Hence a measurement of a leads to an estimate of h and Bi, and determines whether the fibre can be treated as a 1-D system. a constitutes a system time constant, therefore we must measure the filter's wavelength shift in response to a sudden current input.

There is no analytic solution to equation (7), however assuming a step increase in current applied to the metal coating at time $t = 0$ leads to [38]

$$T(x,t) = T_{air} + \frac{1}{2\sqrt{\pi\kappa}} \int_{-\infty}^{+\infty} P_{in}'(z) \int_o^t \frac{1}{\sqrt{\tau}} \exp\left(-a\tau - \frac{(x-z)^2}{4\kappa\tau}\right) dz\,d\tau \qquad (13)$$

which requires numerical integration to evaluate $T(x,t)$ for a given input power $P_{in}(x)$, the heating power/unit length at position x. $P_{in}'(x,t)$ is related to the input power, but depends on the thermal capacity of the PMMA that determines the heat loss of the system.

$$P_{in}'(x,t) = \frac{P_{in}(x,t)}{\rho c_p \pi R_{fibre}^2} \qquad (14)$$

If we assume a uniform input power, the temperature variation is reduced to

$$T(t) = \frac{P_{in}}{a\rho c_p \pi R_{fibre}^2 L}[1 - \exp(-at)] \qquad (15)$$

where the role of the heated fibre volume is clearly evident. For times $t \gg 1/a$ we arrive at a simple form for the temperature increase that can be subsequently related to the Bragg wavelength shift, $\Delta\lambda_B$. The steady state Bragg shift varies according to [15]

$$\Delta\lambda_B = 2\Lambda_B(\tilde{n}\alpha_e + \beta)\Delta T \,\big|_{t\to\infty} \qquad (16)$$

where Λ_B is the period of the Bragg grating, $\tilde{n}$ is the average fibre index at the grating location, α_e is the expansion coefficient and β the thermo-optic coefficient. In the case of silica fibre one can typically ignore α_e as it is an order of magnitude less than β, and we note that the sum of these two contributions results in a positive index shift with temperature for a typical silica-based Type 1 Bragg grating [15]. For PMMA, α_e and β are typically [39] (for the temperature excursion in this work) = 70×10^{-6} K^{-1} and $\beta = -1.2\times10^{-4}$ K^{-1}, with $\tilde{n} = 1.478$ at the Bragg wavelength. Clearly for PMMA one cannot ignore and the large negative thermo-optic coefficient, a consequence of temperature-induced density changes, which lead to a blue shift for $\Delta\lambda_B$ with temperature that is driven by the heating power,

$$\Delta\lambda_B = \frac{2\Lambda_B(\tilde{n}\alpha_e + \beta)P_{in}}{a\rho c_p \pi R_{fibre}^2 L} \qquad (17)$$

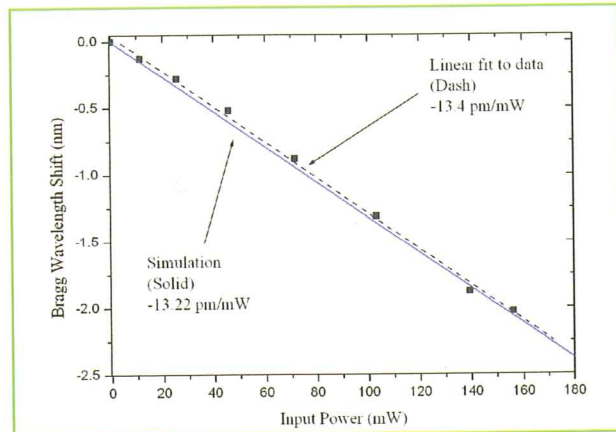*Figure 12.* Wavelength shift via Joule heating with a wavelength to input power coefficient of -13.4 pm mW^{-1} according to a linear fit to the experimental data, and -13.22 pm mW^{-1} simulated using equation (17).
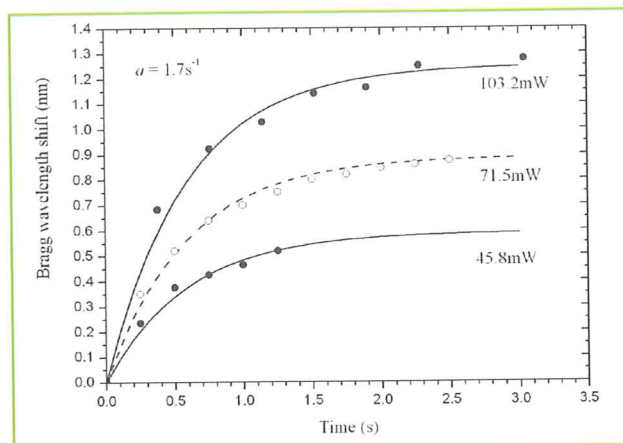

Figure 13. Rise time of a thermally tuned fibre Bragg grating, for heating powers of 45.8, 71.5 and 103.2 mW applied suddenly at $t = 0$ s. The time constant $a = 1.7$ s^{-1}.

7. Results

The tuneable grating filter was characterised via joule heating as current was passed through the thin-film metal coating; changes in wavelength due to current flowing through the thin copper film, were measured using a broadband light source and optical spectrum analyser. The total resistance of the film encompassing the grating, and the connection via copper wires was measured to be 3.2Ω. Figure 12 shows the wavelength shift induced by joule heating, with a negative wavelength to input power coefficient of -13.4 pm/mW according to a linear fit to the experimental data, and -13.22 pm/mW, simulated using equation (17), for which the model shows excellent agreement with the measurements. We have assumed a uniform input power, the phase mask period coincident with the grating inscription, a grating length of 1cm, and the value of a evaluated by fitting equation (15) to the rise-time data. Throughout wavelength tuning the grating spectrum remained unchanged, which is consistent with a spatially uniform heating of the grating.

The measurement of a yields information regarding the rate of heat flow out of the fibre. Figure 13 shows the rise time of a thermally tuned fibre Bragg grating, with data collected for three different heating powers applied suddenly at $t=0$s, 45.8, 71.5, and 103.2mW. The curves correspond to fits that use the single exponential form, from which we have determined the time constant, $a=1.7s^{-1}$. There is no apparent or systematic dependence on the applied power.

Using the geometric and material properties of the fibre ($\rho = 1190$kg/m^3, $c_p = 1450$J/kgK, $R_{fibre} = 120\mu$m, K = 0.17W/mK), h is found to be 175W/m^{2}K, and Bi is ~ 0.1; this is compatible with our initial supposition - a treatment of the polymer fibre as a 1-D system.

8. Conclusions

We have presented a detailed study on the development and successfully demonstrated the first wavelength tuneable fibre Bragg grating filter in POF based on thin-film resistive load heating. The device was coated at room temperature using VUV initiated deposition, this proved important as there was no adverse impact on the grating spectrum and the procedure is well-suited to coating cylindrical polymers with low glass transition temperatures without adversely affecting light guidance. The filter underwent a wavelength shift of 2nm for a moderate input power of 160mW, giving a measured wavelength to input power coefficient of -13.4 pm/mW and time constant of $1.7s^{-1}$. A basic theoretical study verified that for this fibre type one can treat the device as a one dimensional system; the simple model was extended to include the effect of input electrical power changes on the refractive index of the fibre and subsequently to changes in the Bragg wavelength of the grating, the model showing excellent agreement with the experimental measurements. However, the model also indicates that as fibre thickness increases one may have to account for radial gradients across POF based FBG devices.

Acknowledgements

References

[1] Berezhnoi A A 1999 Electro-optical modulators and shutters J. Opt. Technol. 66 583–95

[2] Ackerman E I 1999 Broad-band linearization of a Mach–Zehnder electrooptic modulator IEEE Trans. Microw. Theor. Tech. 47 2271–79

[3] Fox G R, Muller C A P and Setter N 1996 Sputter deposited piezoelectric fiber coatings for acousto-optic modulators J. Vac. Sci. Technol. 14 800–5

[4] Iocco A, Limberger H G, Salathe R P, Everall L A, Chisholm K E, Williams J A R and Bennion I 1999 Bragg grating fast tunable filter for wavelength division multiplexing J. Lightwave Technol. 17 1217–21

[5] Rogers J A, Eggleton B J, Pedrazzani J R and Strasser T A 1999 Distributed on-fiber thin film heaters for Bragg gratings with adjustable chirp Appl. Phys. Lett. 74 3131–3

[6] Eggleton B J, Ahuja A, Westbrook P S, Rogers J A, Kuo P, Nielsen T N and Mikkelsen B 2000 Integrated tunable fiber gratings for dispersion management in high-bit rate systems J. Lightwave Technol. 18 1418–32

[7] Rogers J A, Eggleton B J, Jackman R J, Kowach G R and Strasser T A 1999 Dual on-fiber thin film heaters for fiber gratings with independently adjustable chirp and wavelength Opt. Lett. 24 1328–30

[8] Abramov A A, Eggleton B J, Rogers J A, Espindola R P, Hale A, Windeler R S and Strasser T A 1999 Electrically tunable efficient broad-band fiber filter IEEE Photon. Technol. Lett. 11 445–7

[9] Costantini D M, Muller C A P, Vasiliev S A, Limberger H G and Salathe R P 1999 Tunable loss filter based on metal-coated long-period fiber grating IEEE Photon. Technol. Lett. 11 1458–60

[10] Eggleton B J, Rogers J A, Westbrook P S and Strasser T A 1999 Electrically tunable power efficient dispersion compensating fiber Bragg grating IEEE Photon. Technol. Lett. 11 854–6

[11] Dobb H et al 2006 Grating based devices in polymer optical fibre Proc. SPIE 6189 1–12

[12] Eldada L, Blomquist R, Maxfield M, Pant D, Boudoughian G, Poga C and Norwood R A 1999 Thermooptic planar polymer Bragg grating OADMs with broad tuning range IEEE Photon. Technol. Lett. 11 448–50

[13] van den Boom H P A, Li W, van Bennekom P K, Monroy I T and Khoe G-D 2001 High-capacity transmission over polymer optical fiber IEEE Selected Topics J. Quantum Electron. 7 461–70

[14] Ballato J, Smith D, Foulger S and Wagener E 2002 Theoretical performance of polymer optical fibers, planar waveguides, and amplifiers Proc. SPIE: Design

and Fabrication of Planar Optical Waveguide Devices and Materials vol 4805 pp 1–8

[15] Othonos A and Kalli K 1999 Fiber Bragg Gratings: Fundamentals and Applications in Telecommunications and Sensing (Boston, MA: Artech House)

[16] Tomlinson W J, Kaminow I P, Chandross E A, Forkland R L and Silvfast W T 1970 Photoinduced refractive index increase in poly(methylmethacrylate) and its applications Appl. Phys. Lett. 16 486–9

[17] Chandross E A, Pryde C A, Tomlinson W J and Weber H P 1974 Photolocking—a new technique for fabricating optical waveguide circuits Appl. Phys. Lett. 24 72–4

[18] Bowden M J, Chandross E A and Kaminow I P 1974 Mechanism of the photoinduced refractive index increase in polymethyl methacrylate Appl. Opt. 13 112–17

[19] Moran J and Kaminow I P 1973 Properties of holographic gratings photoinduced in polymethyl methacrylate Appl. Opt. 2 1964–70

[20] Price C C 1946 Mechanism of vinyl polymerizations: IX. Some factors affecting copolymerization J. Polym. Sci. 1 83–9

[21] Barnes C E, Elofson R M and Jones G D 1950 Role of oxygen in vinyl polymerization: II. Isolation and structure of the peroxides of vinyl compounds J. Am. Chem. Soc. 72 210

[22] Colburn W S and Haines K A 1971 Volume hologram formation in photopolymer materials Appl. Opt. 10 1663–41

[23] Xiong Z, Peng G D, Wu B and Chu P L 1999 Highly tunable Bragg gratings in single-mode polymer optical fibers IEEE Photon. Technol. Lett. 11 352–4

[24] Liu H Y, Liu H B, Peng G D and Chu P L 2003 Observation of type I and type II gratings behavior in polymer optical fiber Opt. Commun. 220 337–43

[25] Liu H B, Liu H Y, Peng G D and Chu P L 2003 Strain and temperature sensor using a combination of polymer and silica fibre Bragg gratings Opt. Commun. 219 139–42

[26] Wochnowski C, Metev S and Sepold G 2000 UV-laser-assisted modification of the optical properties of polymethylmethacrylate Appl. Surf. Sci. 154–155 706–11

[27] Baum A, Scully P J, Basanta M, Thomas C L P, Fielden P R, Goddard N J, Perrie W and Chalker P R 2007 Photochemistry of refractive index structures in poly(methyl methacrylate) by femtosecond laser irradiation Opt. Lett. 32 190–2

[28] Peng G D, Chu P L, Lou X and Chaplin R A 1995 Fabrication and characterization of polymer optical fibers J. Electr. Electron. Eng. Aust. 289–96

[29] Liu H Y, Peng G D and Chu P L 2001 Thermal tuning of polymer optical fiber Bragg gratings IEEE Photon. Technol. Lett. 13 824–6

[30] Liu H Y, Peng G D and Chu P L 2002 Polymer fiber Bragg gratings with 28-dB transmission rejection IEEE Photon. Technol. Lett. 14 935–7

[31] Dragomir N M, Rollinson C, Wade S A, Stevenson A J, Collins S F, Baxter G W, Farrell P M and Roberts A 2003 Nondestructive imaging of a type I optical fiber Bragg grating Opt. Lett. 28 789–91

[32] Rahman B M A and Davies J B 1984 Finite-element solution of integrated optical waveguides J. Lightwave Technol. 2 682–8

[33] Ishigure T, Nihei E and Koike Y 1996 Optimum refractive-index profile of the graded-index polymer optical fiber, toward gigabit data links Appl. Opt. 35 2048–53

[34] Yariv A 1973 Coupled-mode theory for guided-wave optics IEEE J. Quantum Electron QE-9 919–33

[35] Erdogan T 1997 Fiber grating spectra J. Lightwave Technol. 15 1277–94

[36] Muriel M A and Carballar A 1997 Internal field distributions in fiber Bragg gratings IEEE Photon. Technol. Lett. 9 955–7

[37] Kalli K, Dobb H L, Webb D J, Carroll K, Komodromos M, Themistos C, Peng G D, Fang Q and Boyd I W 2007 Electrically tunable Bragg gratings in single mode polymer optical fiber Opt. Lett. 32 214–16

[38] Rogers J A, Kuo P, Ahuja A, Eggleton B J and Jackman R J 2000 Characteristics of heat flow in optical fiber devices that use integrated thin-film heaters Appl. Opt. 39 5109–16

[39] Silva-Lopez M, Fender A, MacPherson W N, Barton J S, Jones J D C, Zhao D, Dobb H, Webb D J, Zhang L and Bennion I 2005 Strain and temperature sensitivity of a single-mode polymer optical fiber Opt. Lett. 30 3129–31

USE OF GENETIC ALGORITHMS FOR THE OPTIMUM SELECTION OF FENESTRATION AREA IN BUILDINGS

Soteris A. Kalogirou, Instructor of Mechanical Engineering,
Higher Technical Institute, P. O. Box 20423, Nicosia 2152, Cyprus.

ABSTRACT

The objective of this work is to find the optimum window-to-wall area ratio that minimizes the energy cost for cooling, heating and daylighting. Both heating and cooling load are affected by the U-value and the solar heat gain coefficient (SHGC) of the glass whereas the amount of daylighting is affected by the coefficient of visual transmittance of the glass. For this purpose a genetic algorithm is used which is an optimum search technique based on the concepts of natural selection and survival of the fittest. In this work the genetic algorithm seeks to find a solution which minimizes the energy cost. The method is presented for three different types of fenestration with single glass, double glass and double glass for which the outer glass is reflective. A room with one external 10m² double-brick wall is considered which is the usual case and size for an office room. This is the wall which carries the fenestration and the exercise was performed individually for the four cardinal directions using the weather conditions of Nicosia Cyprus. The results show that for all types of glasses considered the maximum optimum window-to-wall area ratio (WWR) is for the north direction, followed by the west direction whereas the smallest WWR should be in the east direction.

1. INTRODUCTION

A fundamental problem that has to be solved when designing a building is how much window area to use in each direction in order to maximize the use of daylighting but without compromising on the use of heating or air conditioning. Generally, fenestration affects the building cooling load, heating load and daylighting. By increasing the glass area with respect to the wall area, referred to as the window-to-wall area ratio (WWR) increases the cooling and heating loads, whereas the daylighting performance of the building improves thus requiring less electricity for lighting. The studies reported in literature on this subject are very few. A primary source of information is the ASHRAE Handbook of Fundamentals (2005) whereas another study which deals with window size optimization is presented by Marks (1997). Daylight performance under different sky conditions is presented by Wittkopf (2007) whereas the impact of shading design and control is presented by Tzempelikos and Athienitis (2007). The window openings can be used also for passive cooling by cross-ventilation, which affects the building cooling requirements (Nagai, 2006); this issue however is not considered in the present analysis as this is influenced by the occupants' behaviour.

The effects of window size on the thermal load is well known while daylighting is relatively recently considered as a resource for energy conservation. Generally, daylighting is the illumination of the building interiors with sunlight and sky light and is known to affect visual performance, lighting quality, health, human performance and energy efficiency. In some countries there are codes regulating minimum window size, minimum daylight factor

and window position to provide views to all occupants and to create a minimum interior brightness level. In terms of energy efficiency daylighting can provide substantial energy reductions, particularly in non-residential applications through the use of electric lighting controls. Daylight can displace the need for electric lighting at the perimeter zone with vertical windows and at core zone with skylights.

The objective of this work is to find the optimum WWR ratio that minimizes the energy cost for cooling, heating and daylighting. Both heating and cooling load are affected by the U-value and the solar heat gain coefficient (SHGC) of the glass whereas the amount of daylighting is affected by the coefficient of visual transmittance of the glass.

2. GENETIC ALGORITHMS

A Genetic Algorithm (GA) is inspired by the way living organisms adapt to the harsh realities of life in a hostile world. A genetic algorithm is an optimum search technique based on the concepts of natural selection and survival of the fittest. In this work the genetic algorithm used seeks to find a solution which minimizes the energy cost.

Genetic Algorithms are stochastic optimization methods that mimic the process of natural biological evolution. Evolutionary algorithms operate on a population of potential solutions by applying the principle of survival of the fittest to produce better and better approximations to a solution. At each generation, a new set of approximations is created by the process of selecting individuals according to their level of fitness in the problem domain and breeding them together using operators borrowed from natural genetics. This process leads to the evolution of populations of individuals that are better suited to their environment than the individuals that they were created from, just as in natural adaptation. GAs therefore, model natural processes, such as selection, recombination and mutation. Figure 1 shows the structure of a simple genetic algorithm. GAs
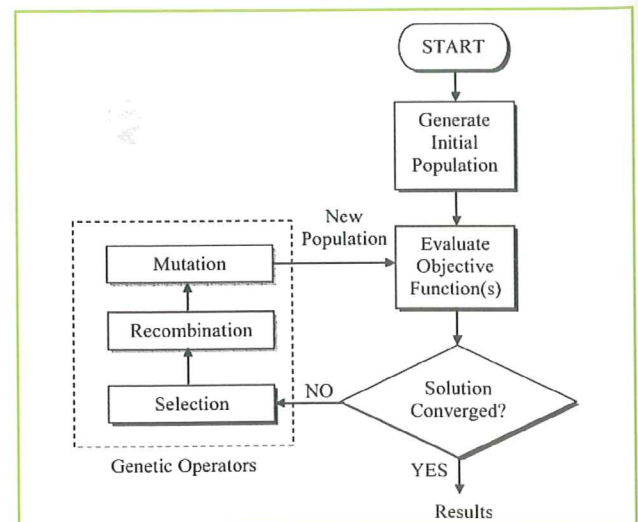

Fig. 1 Problem solution using genetic algorithms

work on populations of individuals instead of single solutions. In this way the search is performed in a parallel manner.

At the beginning of the computation, a number of individuals (the initial population) are randomly initialised. The objective function is then evaluated for these individuals and the first/initial generation is thus produced. If the optimisation criteria are not met the creation of a new generation starts. Individuals are selected according to their fitness for the production of offspring. Parents are recombined to produce offspring.

All offspring will be mutated with a certain probability. The fitness of the offspring is then computed. The offspring are then inserted into the population replacing the old individuals, which in turns produce a new generation. This cycle is performed until the optimization criteria are reached. In the current work, the population consisted of 50 individuals. In the selection process, a generation gap of 0.90 was used, which means that 45 individuals in the old population would be replaced during each optimisation cycle. Finally, the mutation probability coefficient is equal to 0.01. More details on GAs can be found in Zalzala and Fleming (1997), and in Kalogirou (2005).

Genetic algorithms have been widely applied to optimization problems where methods that are more traditional fail. Genetic algorithm (GA) as an optimisation technique is widely used for optimisation of engineering problems. Many engineering design problems are very complex and therefore difficult to solve with conventional optimization techniques (Gen and Cheng, 1997). GAs have been used by the author for the optimal design of solar systems (Kalogirou, 2005).

During the setting up of the GA the user has to specify the adjustable chromosomes, i.e. the parameters that would be modified during evolution to obtain the maximum value of the fitness function. Usually GAs are applied in cases where there are a number of chromosomes (adjustable parameters) which affect the solution of a problem and these are adjusted in order to find the best combination which optimises the problem. In this work however, only one chromosome is used, the WWR. Additionally the user has to specify the range of the WWR values called constraints. In the present work, this constraint is set equal to 0 to 60%.

3. METHOD
The method is presented for three different types of fenestration with single glass, double glass and double glass

for which the outer glass is reflective. Detailed specifications of these assemblies are shown in Table 1. A room with one external 10m2 double-brick wall is considered, which is the usual size for an office room, and the exercise was performed individually for the four cardinal directions using the weather conditions of Nicosia Cyprus. For this purpose the typical meteorological year (TMY) file for Nicosia was used and the horizontal global radiation contained in the TMY was analyzed in the four cardinal directions using the solar radiation processor of TRNSYS (Radiation mode 3, Reindl model).

A representation of the wall/window construction together with the various modes of energy interactions are shown in Fig. 2. As it is indicated in Fig. 2 all other components of the building envelope, i.e., internal walls, floor and ceiling, are considered adiabatic, i.e., they do not contribute to the room thermal load. Fenestration affects both the thermal load (cooling and heating) and daylighting and thus the energy cost (C). In equation form this is given by:

$$C = f (L , D) \tag{1}$$

where:
L = Thermal load (cooling and heating = Qc+Qh)
D = Daylighting.

The loads are estimated every hour. Equation (1) can be further analysed as:

A. Cooling load

The cooling load is given by:

$$Qc = Ug.Ag.\Delta T + Uw.Aw.\Delta T + I.SHGC.Ag \tag{2}$$

where:
I = Solar radiation (W/m^2),
SHGC = Solar heat gain coefficient,
A = Area (m^2)
ΔT = Temperature difference between ambient temperature and required room temperature (°C).

In the present work, the room temperature considered for cooling is 25°C. The subscripts g and w stand for glass and wall respectively. The first two factors of Eq. (2) are the transmission losses through the window and the wall whereas the last one is the direct solar gain entering the room through the window. In this work, it is assumed that no internal curtains are used.

Table 1 Window properties considered

Number of glasses	Type of glass	Glass thickness (mm)	Type of gas	Gas thickness (mm)	U-value (W/m²K)	SHGC	Vt
1	Clear	6	-	-	6.42	0.74	0.79
2	Both clear	6	Air	12	3.61	0.63	0.69
2	Inside clear Outside reflective	6	Air 5%, Argon 95%	12.7	3.08	0.46	0.42

Notes: 1. SHGC = solar heat gain coefficient, 2. Vt = visual transmittance

work on populations of individuals instead of single solutions. In this way the search is performed in a parallel manner.

At the beginning of the computation, a number of individuals (the initial population) are randomly initialised. The objective function is then evaluated for these individuals and the first/initial generation is thus produced. If the optimisation criteria are not met the creation of a new generation starts. Individuals are selected according to their fitness for the production of offspring. Parents are recombined to produce offspring.

All offspring will be mutated with a certain probability. The fitness of the offspring is then computed. The offspring are then inserted into the population replacing the old individuals, which in turns produce a new generation. This cycle is performed until the optimization criteria are reached. In the current work, the population consisted of 50 individuals. In the selection process, a generation gap of 0.90 was used, which means that 45 individuals in the old population would be replaced during each optimisation cycle. Finally, the mutation probability coefficient is equal to 0.01. More details on GAs can be found in Zalzala and Fleming (1997), and in Kalogirou (2005).

Genetic algorithms have been widely applied to optimization problems where methods that are more traditional fail. Genetic algorithm (GA) as an optimisation technique is widely used for optimisation of engineering problems. Many engineering design problems are very complex and therefore difficult to solve with conventional optimization techniques (Gen and Cheng, 1997). GAs have been used by the author for the optimal design of solar systems (Kalogirou, 2005).

During the setting up of the GA the user has to specify the adjustable chromosomes, i.e. the parameters that would be modified during evolution to obtain the maximum value of the fitness function. Usually GAs are applied in cases where there are a number of chromosomes (adjustable parameters) which affect the solution of a problem and these are adjusted in order to find the best combination which optimises the problem. In this work however, only one chromosome is used, the WWR. Additionally the user has to specify the range of the WWR values called constraints. In the present work, this constraint is set equal to 0 to 60%.

3. METHOD

The method is presented for three different types of fenestration with single glass, double glass and double glass

for which the outer glass is reflective. Detailed specifications of these assemblies are shown in Table 1. A room with one external 10m2 double-brick wall is considered, which is the usual size for an office room, and the exercise was performed individually for the four cardinal directions using the weather conditions of Nicosia Cyprus. For this purpose the typical meteorological year (TMY) file for Nicosia was used and the horizontal global radiation contained in the TMY was analyzed in the four cardinal directions using the solar radiation processor of TRNSYS (Radiation mode 3, Reindl model).

A representation of the wall/window construction together with the various modes of energy interactions are shown in Fig. 2. As it is indicated in Fig. 2 all other components of the building envelope, i.e., internal walls, floor and ceiling, are considered adiabatic, i.e., they do not contribute to the room thermal load. Fenestration affects both the thermal load (cooling and heating) and daylighting and thus the energy cost (C). In equation form this is given by:

$$C = f\ (\ L\ ,\ D\ ) \qquad (1)$$

where:
L = Thermal load (cooling and heating = Qc+Qh)
D = Daylighting.

The loads are estimated every hour. Equation (1) can be further analysed as:

A. Cooling load

The cooling load is given by:

$$Qc = Ug.Ag.\Delta T + Uw.Aw.\Delta T + I.SHGC.Ag \qquad (2)$$

where:
I = Solar radiation (W/m^2),
SHGC = Solar heat gain coefficient,
A = Area (m^2)
ΔT = Temperature difference between ambient temperature and required room temperature (°C).

In the present work, the room temperature considered for cooling is 25°C. The subscripts g and w stand for glass and wall respectively. The first two factors of Eq. (2) are the transmission losses through the window and the wall whereas the last one is the direct solar gain entering the room through the window. In this work, it is assumed that no internal curtains are used.

Table 1 Window properties considered

Number of glasses	Type of glass	Glass thickness (mm)	Type of gas	Gas thickness (mm)	U-value (W/m²K)	SHGC	Vt
1	Clear	6	-	-	6.42	0.74	0.79
2	Both clear	6	Air	12	3.61	0.63	0.69
2	Inside clear Outside reflective	6	Air 5%, Argon 95%	12.7	3.08	0.46	0.42

Notes: 1. SHGC = solar heat gain coefficient, 2. Vt = visual transmittance

USE OF GENETIC ALGORITHMS FOR THE OPTIMUM SELECTION OF FENESTRATION AREA IN BUILDINGS

Soteris A. Kalogirou, Instructor of Mechanical Engineering,
Higher Technical Institute, P. O. Box 20423, Nicosia 2152, Cyprus.

ABSTRACT

The objective of this work is to find the optimum window-to-wall area ratio that minimizes the energy cost for cooling, heating and daylighting. Both heating and cooling load are affected by the U-value and the solar heat gain coefficient (SHGC) of the glass whereas the amount of daylighting is affected by the coefficient of visual transmittance of the glass. For this purpose a genetic algorithm is used which is an optimum search technique based on the concepts of natural selection and survival of the fittest. In this work the genetic algorithm seeks to find a solution which minimizes the energy cost. The method is presented for three different types of fenestration with single glass, double glass and double glass for which the outer glass is reflective. A room with one external 10m² double-brick wall is considered which is the usual case and size for an office room. This is the wall which carries the fenestration and the exercise was performed individually for the four cardinal directions using the weather conditions of Nicosia Cyprus. The results show that for all types of glasses considered the maximum optimum window-to-wall area ratio (WWR) is for the north direction, followed by the west direction whereas the smallest WWR should be in the east direction.

1. INTRODUCTION

A fundamental problem that has to be solved when designing a building is how much window area to use in each direction in order to maximize the use of daylighting but without compromising on the use of heating or air conditioning. Generally, fenestration affects the building cooling load, heating load and daylighting. By increasing the glass area with respect to the wall area, referred to as the window-to-wall area ratio (WWR) increases the cooling and heating loads, whereas the daylighting performance of the building improves thus requiring less electricity for lighting. The studies reported in literature on this subject are very few. A primary source of information is the ASHRAE Handbook of Fundamentals (2005) whereas another study which deals with window size optimization is presented by Marks (1997). Daylight performance under different sky conditions is presented by Wittkopf (2007) whereas the impact of shading design and control is presented by Tzempelikos and Athienitis (2007). The window openings can be used also for passive cooling by cross-ventilation, which affects the building cooling requirements (Nagai, 2006); this issue however is not considered in the present analysis as this is influenced by the occupants' behaviour.

The effects of window size on the thermal load is well known while daylighting is relatively recently considered as a resource for energy conservation. Generally, daylighting is the illumination of the building interiors with sunlight and sky light and is known to affect visual performance, lighting quality, health, human performance and energy efficiency. In some countries there are codes regulating minimum window size, minimum daylight factor

and window position to provide views to all occupants and to create a minimum interior brightness level. In terms of energy efficiency daylighting can provide substantial energy reductions, particularly in non-residential applications through the use of electric lighting controls. Daylight can displace the need for electric lighting at the perimeter zone with vertical windows and at core zone with skylights.

The objective of this work is to find the optimum WWR ratio that minimizes the energy cost for cooling, heating and daylighting. Both heating and cooling load are affected by the U-value and the solar heat gain coefficient (SHGC) of the glass whereas the amount of daylighting is affected by the coefficient of visual transmittance of the glass.

2. GENETIC ALGORITHMS

A Genetic Algorithm (GA) is inspired by the way living organisms adapt to the harsh realities of life in a hostile world. A genetic algorithm is an optimum search technique based on the concepts of natural selection and survival of the fittest. In this work the genetic algorithm used seeks to find a solution which minimizes the energy cost.

Genetic Algorithms are stochastic optimization methods that mimic the process of natural biological evolution. Evolutionary algorithms operate on a population of potential solutions by applying the principle of survival of the fittest to produce better and better approximations to a solution. At each generation, a new set of approximations is created by the process of selecting individuals according to their level of fitness in the problem domain and breeding them together using operators borrowed from natural genetics. This process leads to the evolution of populations of individuals that are better suited to their environment than the individuals that they were created from, just as in natural adaptation. GAs therefore, model natural processes, such as selection, recombination and mutation. Figure 1 shows the structure of a simple genetic algorithm. GAs
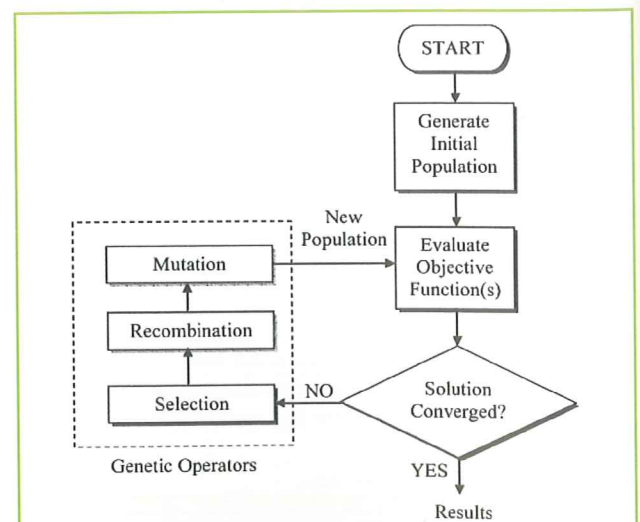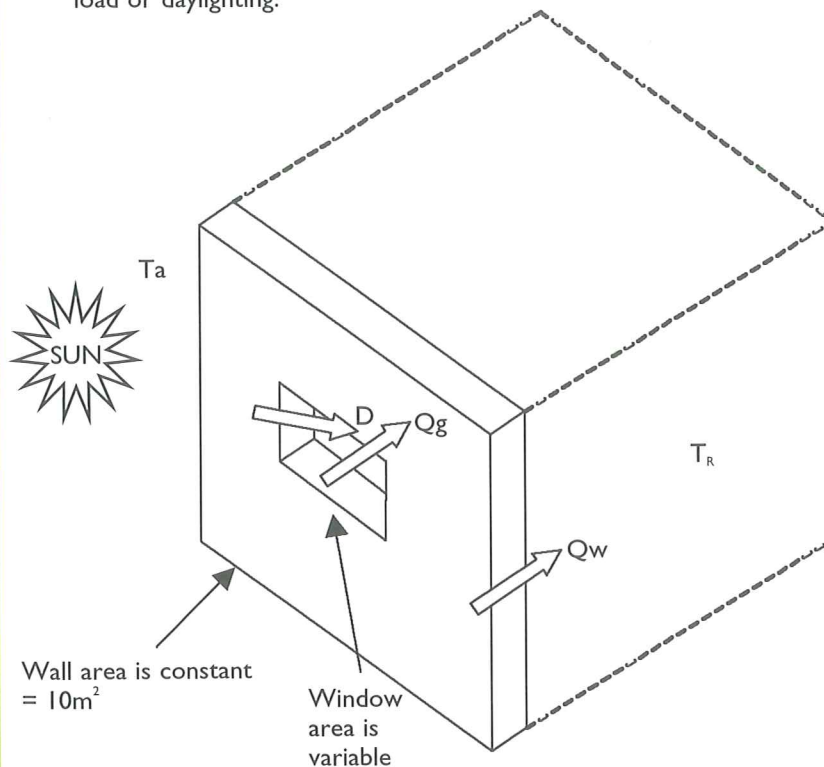

Fig. 1 Problem solution using genetic algorithms

Walls, roof and floor are considered adiabatic, i.e. they do not contribute to the room load or daylighting.

Problem: A bigger size window will create more cooling load, due to higher transmission losses and higher direct solar gains, will create higher heating transmission losses, but it will also allow more direct sunlight to enter the room which will be a gain during winter and have a bigger daylighting effect.

Thus there is a need to optimize the window to wall ratio.

Notes:
1. Room is rotated to face perpendicularly for all four cardinal directions.
2. Loads Qg and Qw include both heating and cooling loads
3. No external or internal shading is considered

Ta

SUN

D Qg

T_R

Qw

Wall area is constant = 10m^2

Window area is variable

Fig.. 2 Schematic representation of the wall-window construction

B. Heating load

The heating load is given by:

$$Qh = Ug.Ag.\Delta T + Uw.Aw.\Delta T - I.SHGC.Ag \qquad (3)$$

All components are the same as in the previous case but the last component is not a loss in this case but a gain as it contributes to the reduction of the heating load. In the present work the room temperature (T_R) considered for heating 20°C.

C. Daylighting

The equation for daylighting, by considering a minimum rate of lighting Rv, is given by:

$$D = Vt . Ag . I – Rv \qquad (4)$$

where:
Vt = Visual transmittance
Rv = Required light intensity in the room which can be taken for handbooks. In the present work a value of 10W/m^2 is considered, which corresponds to 100 W for a 10m^2 floor area room.

The hours of the day during which heating, cooling and daylighting loads are considered are from 8.00-17.00. The various factors used in this work are shown in Table 2.

Table 2 Room properties used in the optimization exercise

Parameter	Symbol	Value
Solar radiation	I	Taken from TMY
Solar heat gain coefficient	SHGC	Taken from Table 1
Glass area	Ag	Variable
Glass U-value	Ug	Taken from Table 1
Wall area	Aw	Variable
Wall U-value	Uw	1.5 W/m^2-°C
Visual transmittance	Vt	Taken from Table 1
Required light intensity	Rv	100 W (=10 W/m^2*10m^2)

The energy sources considered are electricity for the cooling and daylighting and diesel for the heating. For the cooling a COP of the cooling system equal to 2.1 is considered whereas the efficiency of the boiler was equal to 85%. All loads are summed over the year and the totals are multiplied with the appropriate efficiency and cost of the energy source considered. The price of electricity considered is equal to 0.12 €/kWh whereas the price of diesel is 0.73 €/lt (0.0702 €/kWh), which are the current prices in Cyprus.

The objective here is to find the optimum Ag/Aw ratio (adjustable chromosome), mentioned before as WWR, which minimizes the energy cost C. For this purpose the energy loss or gain for the various modes of heat trans-

Constants:	Value
SHGC	0.74
Ug	6.42
Vt	0.79
Cooling room temp.	25°C
Heating room temp.	20°C
RV	100 W
Uw	1.5 W/m²-°C

WWR = [10.79] %   (adjustable chromosome)

Total energy cost = [40.2531] €   (fitness function)

Energy Estimation:

Time	Radiation	Ambient temp.	Cooling load	Heating load	Daylighting
1	0	7.5	0	0	0
2	0	7.0	0	0	0
...	...	...	..	......	...
8760	0	2.0	0	0	0
Totals (Wh):			386,849	98,325	85,798

Fig. 3 Representation of the spreadsheet used for the optimization exercise

fer are estimated every hour and from the total annual values the cost of energy is estimated as explained above. The whole model was set in a spreadsheet program in which the various parameters and equations are entered into different cells (see Fig. 3). As can be seen from Fig. 3, the adjustable chromosome (Ag/Aw ratio) is set in a different cell and the fitness function is the cell that contains an equation giving the total energy cost. During the execution of the program the genetic algorithm tries to find a value of the adjustable chromosome which minimizes the fitness function (total energy cost). For each new value of the chromosome, the spreadsheet is recalculated automatically. It should be noted that, the spreadsheet file described here needs to be constructed once. The only changes required for different problems would be to modify the cells with the window properties and the column of the solar radiation values.

In Fig. 3, the total energy cost in € is estimated from:

$$\text{Energy Cost} = [Qc(annual)/2.1] \cdot 0.12 + [Qh(annual)/0.85] \cdot 0.0702 + D(annual) \cdot 0.12 \qquad (5)$$

The constrain used is that WWR values vary between 0 and 60%. The run time of genetic algorithm and how quickly reaches the minimum solution depends on the initial conditions employed. Generally the run-time is about 2 minutes on a Pentium 3.2 GHz machine. The error recorded by using an initial WWR equal to 3.5% for a single glazing in the north direction is shown in Fig. 4. As can be seen the GA focuses on the optimum solution very fast. The optimum solution is reached after 10 generations whereas a solution very near to the optimum is reached from the 7th generation. The value indicated on the graph is the cost of energy for heating cooling and daylighting for the room for one year.

It should be noted that the GA was set to give the final solution after the minimum solution remained unchanged for 30 generations.
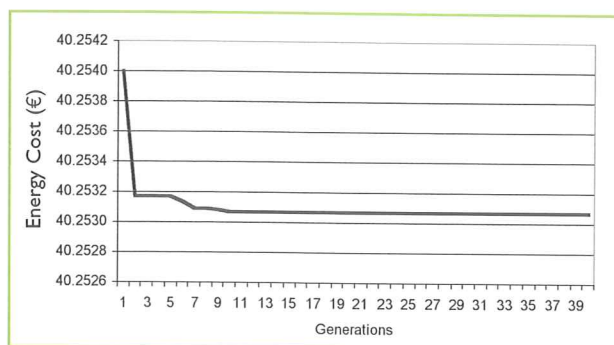

Fig. 4 Plot of best fitness against the number of generations

The results for all types of glasses considered are shown in Table 2. These show that the maximum optimum window-to-wall area ratio (WWR) is for the north direction, followed by the west direction whereas the smallest WWR should be used in the east direction. As can be seen generally the better the glass the larger the area that can be used. As a general conclusion it can be said that glazing must be avoided or used with care in the south and east directions of a building.

Table 2 Results of the optimization

Single glass	
Direction	WWR (%)
S	3.80
E	2.84
W	8.59
N	10.79
Double glass (both glasses clear)	
Direction	WWR (%)
S	4.58
E	3.47
W	10.80
N	13.85
Double glass (inside glass clear, outside reflective)	
Direction	WWR (%)
S	6.42
E	4.93
W	15.09
N	19.86
Note: Wall area = 10 m²	

4. CONCLUSIONS

In this paper a method to find the optimum window-to-wall area ratio that minimizes the energy cost for cooling, heating and daylighting is presented. A genetic algorithm is used for this purpose, which is an optimum search technique based on the concepts of natural selection and survival of the fittest. The method is presented for three different types of fenestration with single glass, double glass and double glass for which the outer glass is reflective. The exercise was performed individually for the four cardinal directions using the weather conditions of Nicosia, Cyprus. The results show that for all types of glasses considered the maximum optimum window-to-wall area ratio (WWR) is for the north direction, followed by the west direction whereas the smallest WWR should be used in the east direction. In fact the glazing in the south and east directions of a building affect to a large extent the thermal characteristics of buildings and must be used with care to avoid unnecessary thermal loads.

REFERENCES

ASHRAE Handbook of Fundamentals (2005). Chapter 31, pp. 31.56-31.59.
Gen M. and Cheng R. (1997). Genetic Algorithms and Engineering Design, London, Wiley.
Kalogirou S. (2005). Use of Artificial Intelligence for the Optimal Design of Solar Systems, *International Journal of Computer Applications in Technology*, Special Issue on *Intelligent Systems for Intelligent Energy in the New Millennium*, Vol. 22, No. 2-3, pp. 90-103.
Marks W. (1997). Multicriteria optimisation of shape of energy-saving buildings, *Building and Environment*, Vol. 32, No. 4, pp. 331-339.
Nagai T. (2006). Windows and HVAC operation to reduce cooling requirement by means of cross-ventilation, *International Journal of Ventilation*, Vol. 5, No. 1, pp. 151-162.
Tzempelikos A. and Athienitis A.K. (2007). The impact of shading design and control on building cooling and lighting demand, *Solar Energy*, Vol. 81, No. 3, pp. 369-382.
Wittkopf S.K., (2007). Daylight performance of anidolic ceiling under different sky condition, *Solar Energy*, Vol. 81, No. 2, pp. 151-161.
Zalzala A. and Fleming P. (1997). Genetic Algorithms in Engineering Systems, *The Institution of Electrical Engineers*, London, UK.

WEALTH VERSUS TECHNICAL EDUCATION AND TRAINING

Dr Lazaros Lazaris, Higher Technical Institute, Mechanical Engineering Department, P.O.Box 20423, 2152 Nicosia.

A paper outlining the importance of education and training, in the creation of wealth and prosperity of a community and the country as a whole.

Wealth is generally perceived by the individual as a stylish car, a luxurious home and many other "social status" related belongings. However, one has to look at wealth as the overall social well-being of a country or state.

As Dr A Denton stated, "wealth is the framework in which citizens through their skills and endeavors can generate a good and healthy lifestyle". Or as Professor Ernest Shannon said, "The ability to make available to people clothing, shelter, transport and communications together with staple things of life such as clean air, food and drink".

More specifically, in developed and developing nations alike, the creation of wealth is the key to improved living standards in all of its dimensions for the citizen. This is the highest goal of the government and the engineering community. Working together, they can apply technology to achieve lasting improvements in the quality of life. Technology, when properly harnessed, is a powerful force for the advancement of national economies. The critical components in this harnessing are:

- Education, training, productivity and investment
- Receptivity and sensitivity among venture partners
- Selectivity in R&D objectives and directions
- Consideration of environmental and other public concerns.

Each is essential to the creation of wealth. Taken together they form a logical framework that incorporates technical, economic and cultural values: in essence a "road map" for the creation of national wealth that is useful for both developing and developed nations" (Caets).

Some countries start with an immediate advantage by having large indigenous resources, for example Australia with its mineral deposits and Saudi Arabia with its oil resources. Couple this with small populations, and the right ingredients are there for a wealthy society, but even so a proper supporting infrastructure and technical skills must be provided.

Most countries however are not so fortunate (take Cyprus for example), and have to rely on the education, training and communication skills of its people as a "services provider" to create prosperity. As far as education is concerned, our university graduates have to be skilled at both technical and non-technical subjects, have analytical skills and be able to solve problems or handle situations they never met before. They must be able to operate in a team based, multidisciplinary world where communication skills are very important. They must be computer literate, and able to acquire other new skills as they become available during their career. They need to be familiar with the culture, literature and history of other countries (most importantly their neighbours) as well as their own

and speak at least one other language other than their mother tongue. A real challenge indeed for today's education systems.
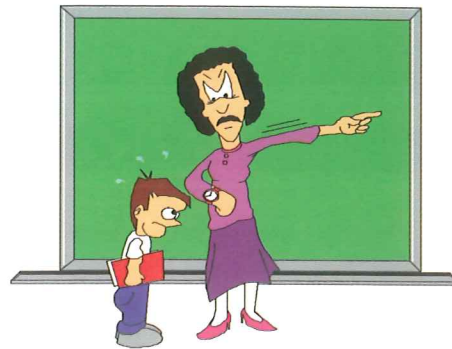
At school we clearly need our young students to be taught well in mathematics, physics, and chemistry. He or she will also need to be exposed to history, geography, art, social economics, languages and of course religious studies (but whether they need 5 or 6 years of any of these subjects is another matter). In my view mathematics is extremely important, and I personally will always be grateful for the excellent tutoring I received in that subject at school.

It is therefore with concern that I see a trend in all educational institutions throughout the world (Cyprus is no exception) towards weakening in the teaching of mathematics. For a significant number of school children and under-graduates we are moving away from teaching what is needed to what is easy to learn (and some would say easy to teach). Differential and integral calculus are the weakest areas. It is worrying to see A-level examination questions today which 10 – 15 years ago were set at O-level. Unless the problem of mathematics teaching is addressed, there is an increasing prospect of our future engineers, for example, using formulae they cannot derive or computer codes they do not understand,

It is perceived as being linked to the tendency not to make children practice their tables by rote. They do not learn that eight eights is 64 until they can picture eight giraffes in eight fields, yet meanwhile struggle with the very basics. A question to all suppliers and receivers of education is: which is better, learning tables by rote at age five and fully understanding the basic framework later, or never understanding the framework and applying formulae by rote at the age of 21?
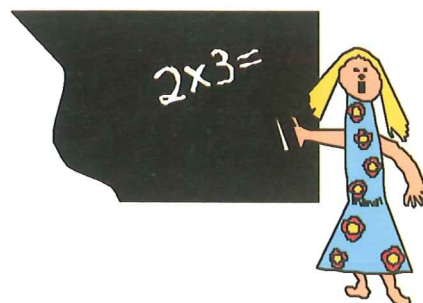
There will be scope for some of those who merely load data into a computer, but good engineering, for example, is about understanding, questioning and being creative. Mathematics is the key tool in this. It may be difficult, but it can be exciting. Merely making it easy is counter-productive.

If one looks at University graduates the situation is becoming increasingly worst. Young people leave High School to continue their studies, at University level, in fields that are of no interest to them and their prospects of employment are minimal if not non-existent. Upon graduation these young people find them-selves unemployed and forced to take employment anywhere to make a living. Within the first 2 – 3 years of trying, without success, to get a descend job they are disheartened, at low spirits and with little or no motivation.

Investing in education is not enough, it has to be coupled with investing in people by providing the means for these young graduates to use their knowledge to develop, create and advance. This way, the investment in education will appear worth while and the contribution to social wealth unquestionable.

Education as a process is no different to any other in the way that it can benefit from quality assurance techniques.

Quality Assurance in teaching can be achieved through:

• Quality control mechanisms within institutions for maintaining and enhancing the quality of their provision.

• Quality audits utilizing external scrutiny aimed to providing guarantees that institutions have suitable quality control in place.

• Validation involving approval courses by validating body for the award of its degrees, diplomas and other qualifications.

• Accreditation of courses by professional institutions.

• Quality assessment through external review of, and judgments about, quality of teaching and learning institutions.

Now education just on its own no matter how well imparted, is insufficient to produce the professional we seek to assist in the wealth creating process, or indeed will be able to meet the demands set by employers. Today employers seek graduates who not only have knowledge, understanding and analytical skills, all of which can be taught, but also experience of how to do things and operate in a team based multidisciplinary world. This brings us to training.

The contribution of engineering, for instance, to the social wealth in Cyprus requires the provision of a supply of technician engineers. Men and women who are intelligent but not of academic bent, and who have manipulative skills must be educated and trained accordingly to exploit their skills. Technical training schools (in tertiary education) have an important role to play in ensuring that such personnel are given a solid grounding in engineering theory and practice, and equipped to communicate. The first employer also has a role in providing company or industry specific tuition. Included in the technician teaching courses there is also a vital need for the inclusion of the teaching of information technology.

Governments have had and will continue to have considerable influence on the well being of their educational systems through their attitude on higher and tertiary education and through their support on training and development.

In conclusion, a systematic collaboration of all interested parties with their respective government in the setting up of effective mechanisms and procedures for the promotion of education and training will gradually set in motion the process of wealth creation for the common good.

READING SCIENCE

Anastasia Mouskou-Peck
Lecturer of English and Report Writing
General Studies Department

Students in any Technological University throughout their studies and later on in their careers will be required to make sense of a range of technical subjects (i.e. Surveying, Strength of Materials, Structural Engineering, Technical Drawing, etc.), as well as topics falling under the heading of science, such as Physics, Mathematics and so on.

In certain university contexts where practical experience is not a major part of the curriculum, unlike the case in the Higher Technical Institute, the emphasis is likely to fall on theory rather than practice. If the main purposes of Technological Universities - and certainly these are the aims of the newly formulated Technological University in Cyprus - are the promotion of science, knowledge, learning and education in the areas of applied sciences and arts through the means of instruction and research, then strong linguistic skills are required. Additionally if the aims of these Universities are to establish themselves as an international educational pole of instruction and research among neighbouring and other countries, as well as develop co-operation with academic and scientific centres abroad then undeniably strong foreign language skills are also needed. This high aspiration demands not only comprehensive scientific and technical input but additional skills on the part of the Institution and its learners, abilities which as already mentioned are to a great extent linguistic and have to do with language requirements, just as much as with scientific context. Therefore, learners will have to develop those skills that will facilitate their learning, both in terms of the activity itself as well as preferably taught in a language which will highly assist this effort, in all likelihood English.

I would like at this point to attempt to make a basic distinction between *science and technology* as this will be running throughout this article. Undoubtedly science and technology are closely entwined, but they differ in the sense that they function differently and are used to produce particular kinds of knowledge or processes.

"The purpose of science is to try to make sense of our environment, whereas technology's purpose is to satisfy our needs (and wants) through making things (such as sliced bread) or developing processes (such as keyhole surgery). Nowadays they are so interdependent that it is not easy to see this essential difference". (Ross, K., Lakin, L., Callaghan, P. 2004:3).

While a scientist is doing the research and has to push the frontier of science and knowledge forward with the formation of theories, the technician is asked to utilize this knowledge and produce various artefacts and processes. The emphasis of the new Technological University in Cyprus would ideally have to be on both theory and practice, thus bringing closely together science and technology. The practical aspect of the curriculum cannot be put to full force without the theoretical / scientific background. Therefore, there will be an extreme need created for the student to be able to read fluently and accurately a variety of texts, which as previously discussed will very likely be written in English.

One neglected activity in the science classroom is *reading*. Obviously, in the course of a school session, the actual amount of reading is very little, and is restricted to perhaps reading notes from the blackboard or the over-head projector, or following instructions from science books and manuals. In fact, Lunzer and Gardener (1979), in a major study of reading across the curriculum (quoted by Wellington & Osborne 2001:41), recorded that only about 10% of the classroom science time was actually spent on reading.

The aim of this article is to present an argument of how important reading is for the new scientist, particularly once a student has left the science classroom. Being able to read effectively and extensively is a major scientific activity; an activity - and by extension ability – which is carried through one's whole future life.

As already presented in previous HTI Review articles, the Internet, and more generally technology, has made text and information more readily accessible than ever before. Therefore the new scientist will be faced with a multitude of scientific textbooks, researches, journals, CD ROMs, reports, articles, which he will be asked to consider and evaluate for himself.

"The ability to read about science carefully, critically and with healthy scepticism is a key element of scientific literacy. Moreover, it is a prerequisite of citizenship and playing a part in a democracy". (Wellington & Osborne 2001:42).

Furthermore, we must never lose sight of the language associated with the majority of this scientific reading, which is no other than English. Therefore difficulty with the language restricts one's reading chances and comprehension. Additionally, apart from possible language difficulties, an about-to-be scientist will need to overcome certain *"stumbling blocks"*, (Wellington & Osborne 2001:43), which are basically linguistic obstacles.
Wellington and Osborne in their research (2001), identified a number of these obstacles:
Initially there are problems with the science vocabulary, which is in itself not easy, since it includes technical words e.g. *(velocity, refraction, anode)*; semi-technical *(emit, component, deflect)*; and non-technical words *(effect, factor, dependent)*.
Also science texts contain a number of *"connectives"*, which are fundamental in drawing conclusions, hypothesizing, and identifying cause and effect. These connectives are not always clearly understood.
Moreover, scientists – unlike journalists – are hesitant and cautious in their use of language and drawing of conclusions, therefore scientific texts are laden with *qualifying* words such as *"most", "the majority of them"* etc.
A further point concerning science texts is that, in their effort to become more approachable and readable, they might have become a bit too colourful and extravagant, containing perhaps too many pictures and glossy colour. Although visuality – much discussed by Kress and Van Leeuwen (2001) - is a major contributing factor in science

comprehension, too much of it might be a hindrance rather than help.

Finally, the science textbook is not exactly fun-reading, since the language associated with it is rather abstract and rigid.

"Because the language of science is expository rather than narrative, it tends to be more turgid, more informa-tion oriented and more succinct than the reading materi-als that children are more used to". (Reid & Hodson (1987), cited in Wellington & Osborne 2001:43).

New scientists will also need to be taught how to be effective readers, by becoming active in their own learn-ing, rather than passive onlookers and solitary learners. This - according to Davies & Greene (1984), cited in Wellington & Osborne 2001:44 – can be done through: firstly, having a purpose, being given a specific goal ; sec-ondly by having a coach – usually the teacher – who offers guidance and direction, and thirdly, by collaborating with other members in a group.

"...passive reading occurs when reading tasks are vague and general rather than specific, and when reading is soli-tary rather than shared. In contrast, active reading involves reading for specific purposes and the sharing of ideas and small-group work". (Wellington & Osborne 2001:45).

In order to assist the science learner's comprehension, certain activities can be put to full use. Lunzer and Gardener (1979), and Davies and Greene (1984), (cited in Wellington & Osborne 2001:45) initially called these DARTs[1]. These activities form two broad categories. Firstly the Reconstruction or Completion DARTs, which mainly include problem solving activities such as: filling in missing words/phrases in a text or diagram, or sequenc-ing information. Secondly the Analysis DARTs, which are mainly activities focusing on locating and categorizing the information in the text. This would include underlining, labeling, recording, constructing, and so on.

A similar strategy to DARTs was devised by Wood (1992), cited in Wellington & Osborne, (2001:51), who suggests practical strategies to guide the reader through the text by providing three levels of comprehension:
The literal level, which involves looking for words and statements appearing in the text.
The interpretive level, involving real comprehension and interpretation of the text, and finally,
The applied level, where students are beginning to put their comprehension into full use, thus making their own evaluations and comparisons. Wood believes that learn-ers should be able to distinguish and apply all three levels progressively.

However, apart from the conventional science textbook, new scientists will have to be made aware of other sources of text available to them.
There is indeed an incredible amount of science present-ed in newspapers and journals which learners will need to approach critically and evaluatively. In doing so the new scientist can satisfy (according to Wellington & Osborne 2001:56), certain objectives such as: 1) He can relate sci-ence to everyday life, and identify the range of sources available in eliciting information and knowledge. 2) He can acquire knowledge of current issues which are topics in "newspaper science", e.g. medicine, the environment, space, food, diet, cloning, pollution, energy sources, waste management and an array of other scientific issues. 3) He can gain a starting point for exploring ideas further, for distinguishing between claims and arguments, and becom-ing aware of scientific controversies. 4) He can be helped to develop economic, industrial, environmental and health consciousness. 5)His critical and active reading, analysis and discussion can be developed and finally 6) He can acquire knowledge and awareness not only of current issues, but realizing also the possible limitations of sci-ence. Similar arguments were made by other researches such as Jarman and Mclune who argued that:

"Newspapers as a resource for teaching and learning about science...almost by definition, they are up-to-date, dealing with current developments in the subject and contemporary issues in society. Indeed, this intrinsic topicality has prompted some to describe newspapers as "living textbooks"...which can lend a particular relevance for their reader." (Jarman & Mclune 2004:186, in Braund & Reiss (eds.,)).

I have tried in this article to briefly outline issues relating to reading science texts with understanding. I have also presented some other potential sources such as newspa-pers that can enable the learner to discover science. Futhermore I have suggested some strategies that could help learners to make sense when reading science. Like any other ability effective reading can only be achieved through systematic teaching and practice. Moreover a learner needs to be a proficient user of language. As already outlined in this article all these strategies and sources can be put to full use by someone who has few language limitations; either in his own native language or more so in a foreign language. Since most of the infor-mation and sources concerning science are offered in another language, and most likely in English, difficulty with English will inevitably lead to difficulty with science.

BIBLIOGRAPHY

Jarman, R. & Mc Clune, B. (2004) " Learning with news-papers", chapter 12 in Braund M. and Reiss M., (eds) **Learning Science Outside the Classroom**, Routledge Falmer

Kress, G. & Van Leeuwen,T. (2001) **Reading images: The Grammar of Visual Design**, Routledge, London and New York

Ross, K., Lakin, L., Callaghan, P. (2004) **Teaching Secondary Science**, 2nd Edition, David Fulton Publishers

Wellington, J. & Osborne, J. (2001) **Language and Literacy in Science Education**, Open University Press, Buckingham, Philadelphia

[1] DARTs = Directed Activities Related to Text (Wellington & Osborne 2001:45).

NEURAL NETWORKS FOR THE IDENTIFICATION OF GAS CYLINDER FAULTS

Costas Neocleous, Senior Lecturer, Mechanical Engineering Department
Higher Technical Institute, P. O. Box 20423, Nicosia, Cyprus, CNeocleous@hti.ac.cy

Constantinos Christodoulou, Laboratory Assistant, Mechanical Engineering Department
Higher Technical Institute, P. O. Box 20423, Nicosia, Cyprus, CChristodoulou@hti.ac.cy

Demos Demosthenous, Director, Intergaz Ltd
Larnaka – Dhekelia Road, Cyprus, intergaz@spidernet.com.cy

Aris Cleanthous, Department of Computer Science, University of Cyprus.
75 Kallipoleos, 1678, P. O. Box 20537, Nicosia, Cyprus, aris.cleanthous@gmail.com

ABSTRACT

The safety of gas cylinders in domestic applications is of utmost importance. A crucial stage in the appraisal of the risk for failures and possible faults is occurring during the filling process. In Cyprus, this task is currently done by specialized workers who monitor the cylinders during filling. In order to explore the possibility for an automated risk appraisal and consequent screening, a system of fault identification using vibrational time series and neural network classification has been used. Two systems have been attempted. One using a multi-slab feedforward neural structure employing backpropagation-type learning, and a Kohonen self-organizing map. The results were also compared with different simple statistical methods. The feedforward net, proved to be slightly better responding than the Kohonen map for this particular problem.

KEY WORDS

Feedforward neural networks, Kohonen network, gas cylinder safety.

1. Introduction.

The monitoring and appraisal of gas cylinder condition in Cyprus, is currently done by dedicated workers who visually observe the moving cylinders in a filling process line. This approach is costly, and sometimes unreliable, especially when it comes to identifying the general corrosion on the underside of the highly corroded cylinders. The cylinders are pressure tested during manufacture and major maintenance, but during the filling process they need to go through a systematic and thorough inspection for any serious faults.

The present study involves the examination of vibrational signatures of individual cylinders in order to appraise their general condition and thus classify them as acceptable or not. The unacceptable ones are properly maintained, provided that this is economically feasible.

The paradigm of neural networks has been used in different attempts for applications in fault classification of different machinery and systems ([1], [2], [3], [4], [5], [6], [7], [8] Lee et al., 2004). Since, though, in many times, the identification of faults has to do with crucial safety issues, there is a need for a highly reliable identifier system.

For the analysis of the signals, both statistical and non-parametric neural techniques have been used. For the neural network classification, two major systems have been attempted. In each of the two major paradigms a number of special cases involving different architectures and learning procedures have been explored.

The most successful structure found, is that of a multi-slab feedforward neural network employing backpropagation type learning. A Kohonen self-organizing map has also been tried but it was slightly less successful compared to the feedforward structure.

Such systems could also be used as support mechanisms to a larger fault identification system that possibly employs human observers. The system studied and presented in this paper is of such a type

2. Instrumentation and data collection.

2.1. Instrumentation set-up.

A total of 63 empty gas cylinders that had their relief valves removed, were excited by a suitable hammer and the response was recorded via a Bruel and Kjaer (B&K) set of instruments as will be explained further on. The experimental set-up is shown in Figure 1.

Figure 1. The gas cylinder experimental set-up.

The cylinders were provided by the INTERGAZ FILLING Co in Cyprus. They were manufactured as per the BS5045 Part 2.2A specification, being of 24 liter capacity. They were pressure tested at 30 bar and the working pressure is limited to 20 bars. The tare weight varied between 13.1 kgf to 13.4 kgf.

Fiftyone of the tested cylinders were brand new, while five had a small artificially produced horizontal dent. Three more cylinders were given a small, artificially produced, vertical dent. Finally, four more cylinders were selected to have a general severe corrosion at the bottom.

The instrumentation used was based on the (B&K) multichannel analyzer type 3550. The analyzer had many capabilities for signal processing, such as for spectrum averaging, 1/n octave spectrum averaging, zero pad, time capturing, time history, amplitude probability. The associated units that were used in the measurements were a charge amplifier type 2635, a noise generator type 1405, a power amplifier type 2706, an accelerometer type 4370, a vibration exciter type 4809, and an impact hammer type 8202, all from the (B&K) group.

Table 1. Set-up parameters

PARAMETERS	SET-UP
Mode of measurement	Frequency response
Estimator of measurement	H2
Averaging of measurements	Every Peak 10
Trigger	Signal X1
Frequency span (kHz)	6.4 kHz
Δf (Hz)	8 Hz
T (ms)	125 ms
Δt (us)	61.0
Weighting of signal Y1	Rectangular

A typical measurement and the associated settings are shown in Figure 2, while the values for the different parameters of the set-up are shown in Table 1.

2.2 Collected data

For each cylinder a frequency response has been obtained. A total of 676 discrete values of frequencies have been collected and processed for each cylinder. Thus the data matrix had a size of 676x63. A typical plot of the measured data, showing the difference in response between "GOOD" and "BAD" cylinders of vertical dent is shown in Figure 3.

3. Statistical fault classification

Different attempts were made to identify simple statistical ways to screen the good cylinders from the bad ones. In one attempt, the measured frequency response signal for each gas cylinder was cut above 4 kHz. The remaining values were then divided into four frequency ranges, namely, 0 – 1 kHz, 1 – 2 kHz, 2 – 3 kHz, 3 – 4 kHz. For each one of these ranges, the peak values were identified.

Following that, the ratio of peaks and the differences of minimum values were plotted in order to try to identify significant differences between the "GOOD" and "BAD" cylinders. Graphs of these results are shown in Figure 4 and Figure 5.

As it can be easily seen, the ratio of peak values was unable to distinguish between the "GOOD' and the "BAD" classes of cylinders. The differences of minimum values method, however, gave some reasonably good results as indicated in Figure 5, but definitely not acceptable for reliable fault identification.
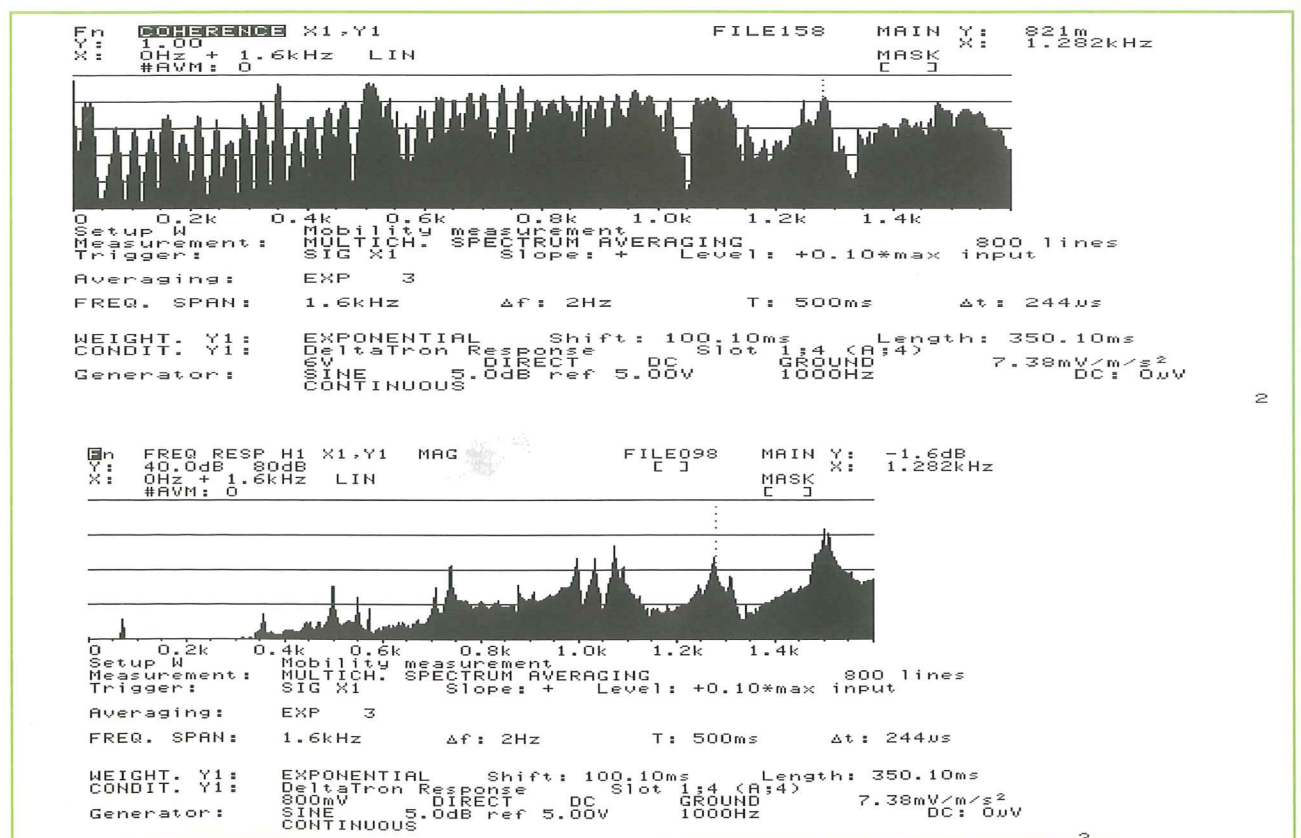

Figure 2. Typical frequency response and coherence of an excited gas cylinder.
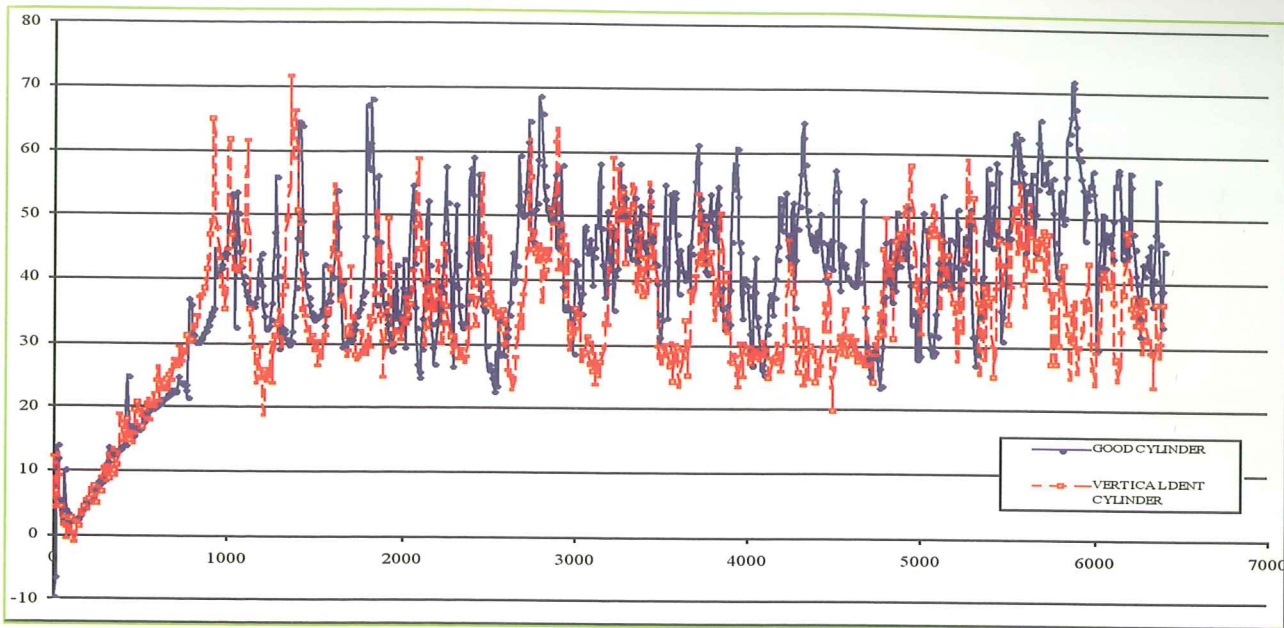
Figure 3. Frequency response of a typical "GOOD" and a typical "BAD" cylinder.
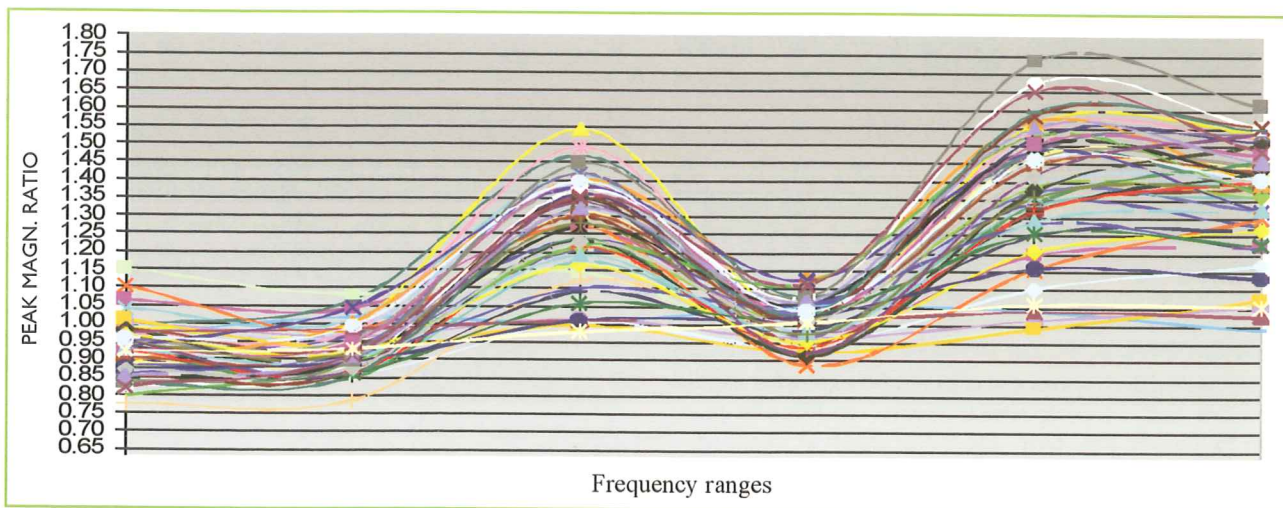

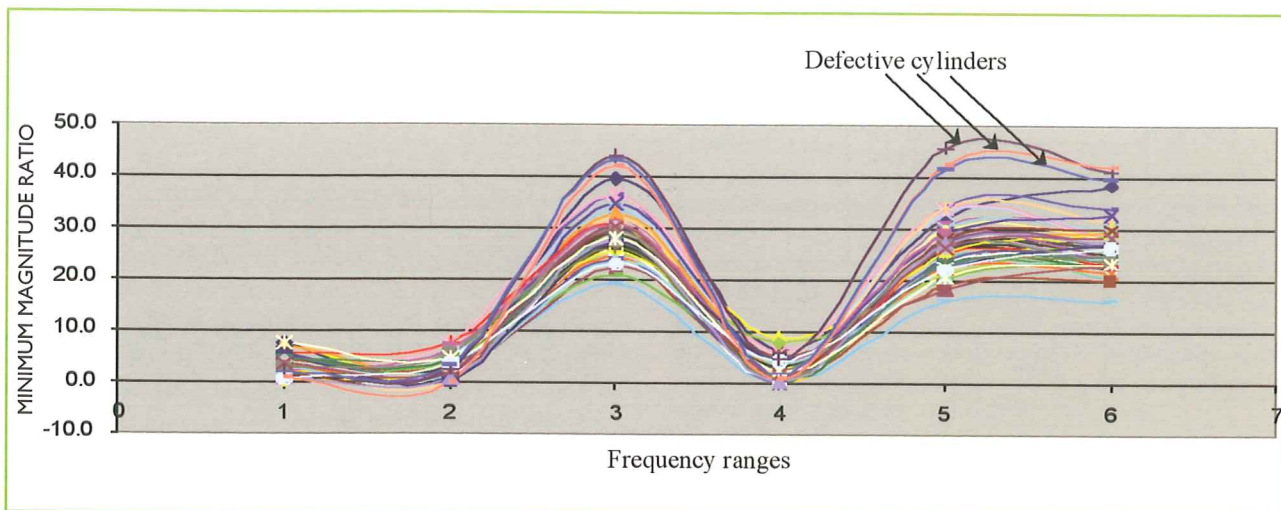Figure 4. Ratio of peak values for the different frequency ranges.

Figure 5. Differences of minimum values for the different frequency ranges.

4. Neural network fault classification

Two systems of neural structures have been attempted. A Kohonen self-organizing map and a multi-slab feedforward architecture using backpropagation-type learning.

4.1 The Kohonen self-organizing map

Standard Kohonen self-organizing maps of different structures and characteristics have been used to help in classifying the "GOOD" and the "BAD" cylinders. The parameters of the best responding network, that was finally used, are given below.

The topology was of a 4x4 network (total of 16 neurons) and the learning of standard Kohonen type. The initial neighborhood size was 2.5 and the initial learning rate 0.1. A total of 30,000 training presentations of 39 (out of 64) representative selections of cylinders were done. Of the 39 cylinders, 30 were of the "GOOD" class and 9 were of the "BAD" class. The "GOOD" and "BAD" samples had an equal exposure of 15,000 presentations each. The remaining 25 cylinders (19 "GOOD" and 6 "BAD") were used only as a test set for verification.

The best results obtained for the unknown test sample were 24 correctly classed (out of 25). Thus a success rate of 96% on the verification set was obtained.

4.2 Multi-slab feedforward architecture

The frequency response at 676 frequency values for the 63 cylinders was first reduced to a smaller size matrix of 67x63 in order to keep the size manageable by the Ward System architecture. This was done by averaging the response for every 10 raw measurements. With such modified data, a WARD 2 multi-slab feedforward neural network structure as shown in Figure 6 was implemented. The selected architecture was based on extensive experience we had on using similar structures [9], and being able to identify the "best" for the problem at hand.
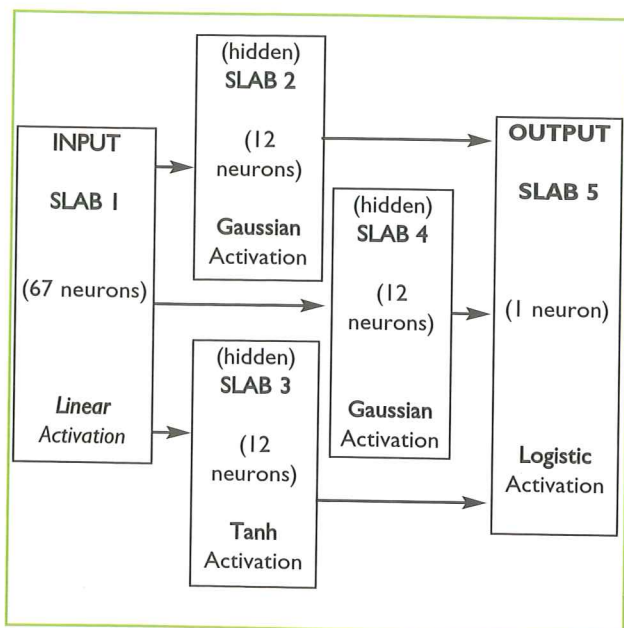

Figure 6. The specific WARD 2 multi-slab feedforward neural architecture used for the simulations.

The learning rate used was 0.1 for all the slabs, while the momentum rate was 0.1. All neurons were initialized at a value of 0.3. During the training of the architecture, 11 representative cylinders (of a mixture of "GOOD" and "BAD" classes) were left out of the training sample to be used for verification. The best results obtained for this structure were 98% correct classifications based on all the cylinder samples and 91% based on the unknown sample of the 11 cylinders.

5. Comparisons and discussion

From the three methodologies used, the multi-slab feedforward structure proved to be slightly better than the Kohonen net. The statistical approaches, as used, were unable to yield a satisfactory screening of the two distinct classes of gas cylinders. Once the method is established and tested in a greater sample, it may also be feasible to test cylinders so that different individual faults may be discriminated.

The research team is presently also examining the possibility of using acoustic signals for fault identification through the use of suitable neural structures. Such an approach will be more economical in implementation. Results will be presented in a future article.

References

[1] T. Sorsa, H. Koivo & H. Koivisto, Neural net-works in process fault diagnosis, IEEE Transac-tions of Systems, Man, Cybernetics, 21(4), 1991, 815—825,

[2] Z. Szewczyk, P. Hajela, Damage detection in structures based on feature sensitive neural net-works, ASCE Journal of Computational Civil Eng., 8, 1994, 163–179.

[3] T. Marwala, H. Hunt, Fault identification using fi-nite element models and neural networks. Mechanical Systems and Signal Processing, 13(3), 1999, 475-490.

[4] T. Marwala, Fault identification using neural net-works and vibration data, (PhD Thesis, University of Cambridge, UK, 2000).

[5] T. Marwala, Probabilistic fault identification using a committee of neural networks and vibration data, J. Aircraft, 38, 2001, 138–146.

[6] Q. Chen, Y. Chan & K. Worden, Structural fault diagnosis and isolation using neural networks based on response only data, Comp. Struct., 81, 2003, 2165–2172.

[7] V. Crupi, E. Guglielmino & G. Milazzo, Neural net-work based system for novel fault detection in rotating machinery, Journal of Vibration and Con-trol, 10(8), 2004, 1137-1150.

[8] I. Lee, J. Kim, J. Lee, Y. Lee & K. Kim, Neural networks based fault detection and isolation of nonlinear systems, Proceeding of Neural Networks and Computational Intelligence, 2004.

[9] C. Neocleous, C. Schizas, Artificial Neural Net-works in Estimating Marine Propeller Cavitation. CDROM Proceedings of the World Congress on Computational Intelligence IJCNN2002, 2002.

LOW ENERGY BUILDING DESIGN
The effectiveness of mass increase

Despina Serghides, AADipl., RIBA II, Grad., Ph.D Architect
Higher Technical Institute
C Kavafi Str., Aglantzia, P.O. Box 20423, 2152 Nicosia, Cyprus.
d.k. serghides@cytanet.com.cy. Tel:+35722406333 Fax:+35722406349

1. INTRODUCTION

This presentation projects the potential application of Bioclimatic Design interwoven with the objective of energy conservation and utilization of renewable energy resources for indoor comfort.

The variable of mass and its effect on other variables and parameters in building simulations are outlined and discussed. The results are computer calculations of building simulations carried out by computer program SERIRES (Ref 1 – 3.2.2.4 "The Simulation models").

The effect of the most important parameters of the variable of mass, on the thermal response of the building is assessed during both heating and cooling modes. The performance of the parameters analysed, their efficiency is compared with each other and their effectiveness is expressed in the constructional aspects for buildings.

Furthermore the adoption of the effectiveness of mass is presented in application of the bioclimatic designs for the Student Housing of New University of Cyprus, for which the presenter is the bioclimatic design consultant.

The presentation is extensively illustrated with slides.

2. SICNIFICANCE OF MASS

The thermal capacity of the building elements determines the heat that can be stored in the envelope of the building. This is an important property of the building envelope for energy conservation, since excess heat is stored in it and dissipated at a later stage when needed. In this way, the indoor temperature fluctuations are regulated and overheating is avoided. These temperature fluctuations could be due to:

• Diurnal fluctuations of outdoor Temperatures
• Internal Gains
• Incident Solar Radiation especially in rooms with large South glazing surfaces

The aspects relating to mass are of particular significance for countries with large diurnal fluctuations and the potential possessed by mass for large solar contribution in winter and cooling in summer by retaining the solar radiation during winter days and the night coolth in summer. This implies that heat admitted during the day in winter could be stored for use during the evening hours and in the summer could be dissipated in the cool night.

3. PARAMETERS

In this research the thermal response of the building and the effectiveness of mass increase are examined internally and externally.

The concept of addition of mass is presented as an acceptable modification of the walls construction in the Cyprus marketplace. The addition of internal mass is introduced as the replacement of the 100mm typical internal brick walls, by 100mm concrete walls. The addition of external mass is introduced by the replacement of the 200mm external brick walls by 200mm concrete walls. (Fig. 3.1. Ref.1.3 "Variables, Varied Parameters – Using Data- Sets"). The studies of addition of mass result at the following percentages regarding energy consumption:

(i) The addition of internal mass yields to 5% reduction of cooling as well as heating load.

(ii) The addition of external mass increases energy consumption by 40%.

A further 30% of internal mass, expressed in the design as additional internal wall, leaves the energy consumption of the house unaffected. This could be attributed to the orientation of the additional mass. A south orientation allows greater insolation in winter and the mass absorbs, stores and dissipates more heat. Another possible reason could be the quantity of the mass. From the studies it appears that the extent of mass increase seems to be critical concerning its effect on the energy loading. Extensive increase of internal mass could act adversely in as far as time needed to cool it in the summer nights or indeed heat it in the winter.
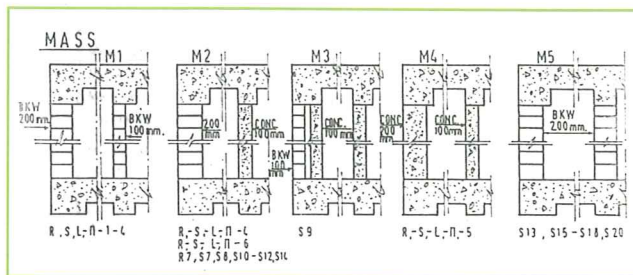
3.1 MASS AND SHAPE

The planning, the design, and the appropriate choice of materials, especially the mass distribution and the location, for these walls, the floors and the other indoor building elements contribute enormously in this. The geometry of the rooms, the building materials and the finishing of the internal surfaces aspecting south, have a bearing on the distribution of the incoming radiation among the room surfaces and affect the attainment, storage and redistribution of solar radiation in the form of heat.

From the building simulation studies it is derived that more complex configurations result to additional factors which intervene in the thermal behaviour of the building. Such additional factors are:

- The more composite internal layout encompassing more spaces and surfaces facing south.
- Larger internal thermal mass whose position, size and distribution reduce temperature fluctuations by retaining heat within it.
- When insulated, enhanced thermal protection on external envelope as a result of the morphology of the two more complex shapes.
- More useful exchanges through openings and surrounding walls.

Furthermore the study has shown that addition of internal mass incurs energy conservation of varied extent according to the thermal behaviour of each shape. On the contrary addition of external mass leads to higher energy consumption in all shapes. Whereas masonry provides good heat storage medium within a space, it readily passes the heat to the outside when added on exterior walls. More analytically, the studies of shape and mass presented the following observations.

(a) Addition of Mass Internally: The addition of internal mass combined with the maximization of south glazing, increases energy conservation in heating for all shapes. The rectangular shape presents the highest amounts of savings. This difference is attributed to the greater extent of south glazing increase on this shape, the positive effect of which was not apparent prior to the mass addition; it seems that the position, the size and distribution of the mass acted positively on energy conservation in heating load when combined with the south glazing increase. The addition of thermal mass also decreased the cooling load in all shapes. The energy reduction is due to the potential of the mass to retain the coolness of the night. When summing up energy consumption in both heating and cooling, it is observed that the square shape retains its lead in being the most economical house. The compactness of the shape seems to overshadow the other tested variables.

(b) Shape and Addition of Mass Externally: The addition of external mass affects adversely the conservation of energy in all four shapes. The replacement of the 20cm external brick wall with 20cm concrete although has greater degree of density, however its thermal conductivity is also greater. During the summer the heat penetrates faster the collective surface and the potential for positive results decreases; consequently the cooling load increases. Based on the same transfer heat principle, in winter the increase of thermal losses results to higher heating demands.

3.2. MASS – IMPROVED DESIGN

The mass variable was also examined on a thermally improved building and the energy savings compared with those incurring from an unimproved structure. The figures of decrease and increase of energy consumption shrunk correspondingly for both the addition of internal and external mass.

Specifically savings from energy conservation increase when insulation is applied on the external surface of the envelope, for both cooling and heating. The interception of the sun at the very external side of the buildings skin in the summer results to the efficiency of external insulation for cooling energy conservation. In the winter with

the positioning of the insulation on the external side, the mass of the opaque elements of the structure is utilized by storing the trapped solar energy contributing to the efficient bioclimatic operation of the building. The insulation on the exterior of envelope prevents heat stored in the thermal mass to be conducted rapidly to the outside.

4. CONCLUSIONS

In order to determine the full extent of the effect of mass on the thermal behaviour of the building further analysis is necessary concerning parameters such as:

(a) Collective and storage characteristics of the materials of the surface finishing.
(b) Location, quantity, distribution and surface colour of mass.
(c) Orientation of internal surfaces.
(d) Diurnal and spatial temperature swings.
(e) Combination of window sizing and extent of thermal mass.

However the mass parameters tested on the current studies were sufficiently indicative as to determine their effect. The addition of internal mass was positive and thus employed as energy conservation measure adopted in building bioclimatic designs.

5. APPLICATION IN THE BIOCLIMATIC DESIGN FOR THE STUDENT HOUSING OF NEW UNIVERSITY OF CYPRUS

In this section effective and beneficial aspects of applications of mass in the buildings as well as in open space elements for the designs of the Student Housing of the New University of Cyprus are presented. The bioclimatic design is consciously integrated into the whole planning, siting and architecture of the scheme.

The siting of the buildings and treatment of open spaces utilises the natural topography and environmental features.

5.1 MASS AND THE BUILDINGS

In all buildings, the shape, the mass, the orientation, the layout and the openings have been designed to meet the conditions of bioclimatic architecture.

The buildings are oriented on East-West axis, to provide for favorable winter solar gain, summer shading, year-round day lighting and natural ventilation. All blocks of buildings feature fixed external passive shading devices. In addition, four of the blocks are beneath a fixed canopy shade, with slats spaced and angled to allow for winter sun exposure and summer sun protection, complementing the passive solar design of the structures. The designs also promote natural summer cooling ventilation, utilizing the prevailing summer wind direction as well as enhancing stack-effect ventilation. These are assisted by rock-bed pre-cooling in the buildings, and rock and screen evaporative cooling structures upwind from the buildings. The buildings on the West Side of the plots, due to the natural contours, are raised at a higher level. The space between the ground and the underside of the buildings is filled with loose rubble stones, encased in metal wire. In
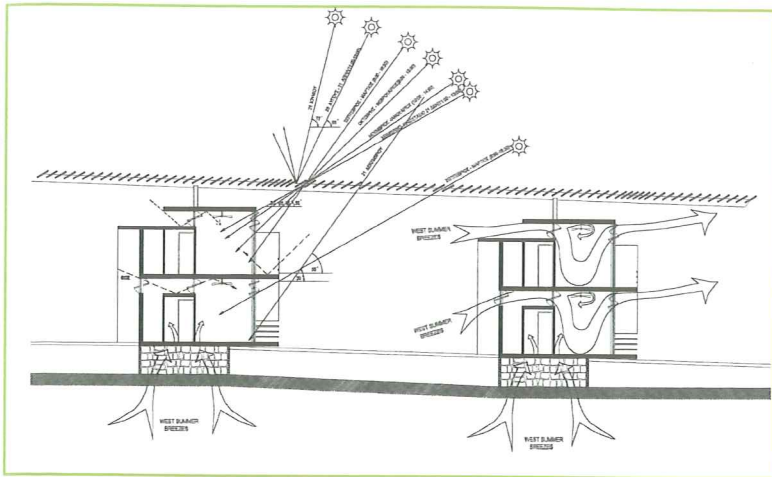
Fig. 5.1. Section views showing, in winter, the sun penetration in the center of the day through the properly angled canopy slats. In summer, direct sun penetration is prevented by the slat angle and spacing. The narrow shape and placement of openings promote natural ventilation. Evaporative cooling from the underfloor wetted rubble stones provides additional summer comfort.

enjoy the warmth of the winter sun. In the summer, open to the clear cold nocturnal sky, they cool by long wave radiation and moderate the heat of the hot days, around them. Within it the open space, which is defined by a circular wall, is pleasant for both summer and winter. It is partly solid toward the northern side for wind protection and the remaining wall and columns are built out of loose rubble stones encased in metal mesh. This is shown in plan view in Fig. 5.2.

In the summer, recycled water trickles through the stones, providing coolness to the adjacent areas. The stone wall and columns are facing the western cool summer breezes to they enhance effectively the cooling of the open and semi-open sitting space. In the winter the stonework is not wetted so that it acts as a wall and columns for solar collection, storage and warmth of the space, which becomes a pleasant sunny courtyard.

the summer it is wetted with water, enhancing the cooling effect of the westerly summer breezes (Fig. 4). Openings in the ground floor insulated and waterproofed slab, channel coolness into the rooms. The free flow of air towards all directions and through the gaps between the stones, under the floor slabs, dissipates coolness in the surrounding areas. It also avoids dampness and creation of mold. The water, which is used for the wetting of the stones, is collected in waterproofed metal trays and is recycled with the aid of a pump, for water conservation. The pumps are activated by an array of photovoltaic panels for solar energy utilization.

The construction of the buildings is of reinforced concrete frame structures with infill panels of concrete blocks, which are locally manufactured. This type of massive construction, in addition to the concrete floor and roof slabs, offers time lag as well as thermal storage. This is of particular significance for the Cyprus climatic conditions, due to the characteristic of large diurnal fluctuations (5 to 25 degrees Celsius) and the potential inherent in mass for large solar contribution in winter and cooling in the night.

The walls are insulated externally with rigid extruded polystyrene and rendered with plaster on plastic mesh painted white for sun reflection.

The concrete floor slabs are finished with screed and mosaic tiles, enhancing their thermal capacity. The concrete roof slabs are topped with lightweight concrete screed forming slopes for water collection, waterproofing membrane and insulation to intercept the summer solar radiation. A protection layer of white chipping acts as a reflecting surface, necessary for the reflection of the almost vertical summer sunrays.

5.2 MASS IN THE OPEN SPACES
The main open space is formed centrally, connected with the building of common spaces and the semi-open route of circulation and parking. It is paved and acts like a large courtyard, sunny in winter and cool in summer. The uncovered paved surfaces offer pleasant sitting areas to
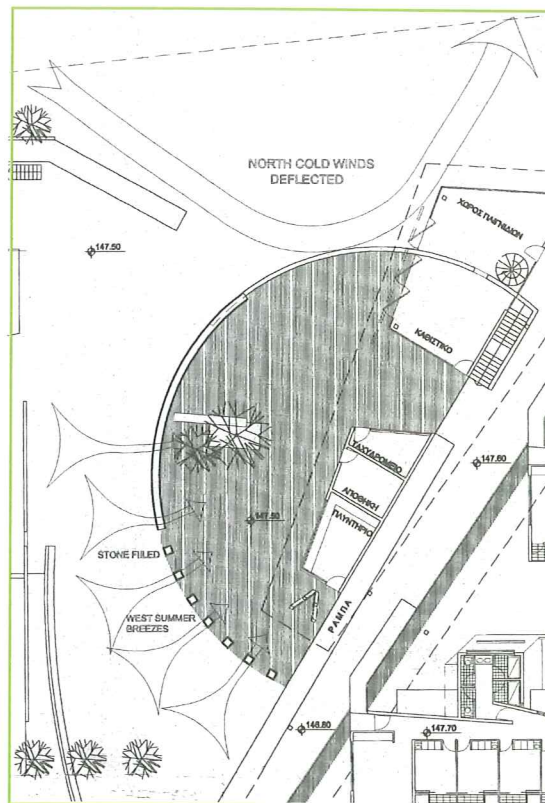

Fig. 5.2 Courtyard defined by circular wall with wetted rubble stone columns for summer evaporative cooling and enhancement of western breezes. In winter the courtyard becomes a pleasant sunny place, warmed by sun and mass

REFERENCES

1. D. K. Serghides 1993 "Zero Energy for the Cyprus House" PhD, Architectural Association, London.

2. D. K. Serghides 1999 "Bioclimatic Designs for the New University of Cyprus Campus" 2nd Competition Phase of Student Housing. ISES-99 Solar World Congress, Jerusalem, Israel-Proceedings.

Participation of Staff in Short Courses/ Conferences and Educational Exchange Programmes for the Academic Year 2006 – 2007

Conferences/ Seminars attended by HTI Academic Staff:

1. Mr. Charalambos Chrysafiades, Senior Lecturer in the Electrical Engineering Department, participated in the **XVII International Conference on Electrical Machines**, in Chania, Greta, 2 – 5 September 2006.

2. Dr Nicos Angastiniotis, Lecturer in the Mechanical Engineering Department, participated in the European **"KMM Integration Conference"** where he presented a research titled: *"Synthesis of Three – Dimensional Multifunctional Building Blocks through Predictive Metastable Particulate Transformations"* in Metz, France, 25 – 26 October 2006.

3. Mr. Theodoros Symeou, Lecturer in the Mechanical Engineering Department and National Secretary of IAESTE Cyprus, attended the **59th Annual Conference of IAESTE**, held in Lisbon, Portugal, 19 – 25 January 2007.

4. Dr Nicholas Kathijotes, Lecturer in the Civil Engineering Department, participated in the National Conference **"Diffuse Inputs into Groundwater"** where he presented a research titled: *"Wastewater Reuse for Irrigation Salinity Risk Evaluation - Prediction"* in Graz, Austria, 29 – 31 January 2007.

5. Dr Pavlos Christodoulides, Lecturer in the General Studies Department, presented a research in the 5th National Conference **"Imacs International Conference on Nonlinear Evolution Equations and Wave Phenomena"** titled: *"Gap-Solitons in a Three-Layer Statified Shear Flow"* in Athens GA, USA, 16 – 19 April 2007.

6. Mr. Charalambos Chrysafiades, Senior Lecturer in the Electrical Engineering Department, participated in the **19th International Conference and Exhibition on Electricity Distribution**, held in Vienna, Austria, 21 – 25 May 2007.

7. Dr Ioannis Angeli, Lecturer in the Mechanical Engineering Department, participated in the **2nd Balkan Quality Forum**, in Belgrade, Serbia, 29 – 30 May 2007.

8. Dr Despina Serghides, Senior Lecturer in the Civil Engineering Department, attended the National Conference **"NorthSun 2007"**, held in Riga, Latvia, 30 May – 1 June 2007.

9. Dr George Florides, Senior Instructor in the Engineering Practice Department and Dr Soteris Kalogirou, Instructor in the Engineering Practice Department, took part in the National Conference **"CLIMA 2007"** where they presented their researches titled: *"Optimization and Cost Analysis of a Lithium Bromide Absorption Solar Cooling System"* and *"Application of the European Directive for the Energy Efficiency of Buildings in Cyprus"* respectively, in Helsinki, Finland, 9 – 14 June 2007.

10. Mr. Savvas Savvides, Head of the Engineering Practice Department, attended the **Annual General Meeting of European Higher Engineering Education and Technical Professionals Association (EurEta)**, held in Stockholm, Sweden, 14 – 17 June 2007.

11. Mr. Spyros Spyrou, Head of the Electrical Engineering Department, attended the European Conference **"MEDICON 2007"**, held in Ljubljana, Slovenia, 26 – 30 June 2007.

12. Dr Nicos Angastiniotis, Lecturer in the Mechanical Engineering Department, attended the National Conference **"NanoSMat – The International Conference on Surfaces, Coatings and Nano-structured Materials"** where he presented the results of his research titled: *"Large Scale Synthesis of Nanomaterial Building Blocks that Deliver Predefined Functionality"*, in Algrave, Portugal, 9 – 11 July 2007.

Short Courses attended by HTI Academic Staff:

1. Dr Kyriacos Kalli, Lecturer in the General Studies Department, participated in the workshop **"Femto – second laser induced gratings in optical fibres"** at Aston University in Birmingham, UK, 6 – 10 November 2006.

2. Mrs. Pola Tsikkou, Lab Assistant in the Computer Studies Department, attended the training program: **"Writing for the Web: Skills for Developing Compelling Content"** which took place in London, 13 – 15 November 2006.

3. Mr. Constantinos Ioannou, Lab Assistant in the Electrical Engineering Department, attended the course: **"RFIC & MMIC – microwave integrated circuits"** at Surrey University, 16 – 20 April 2007.

4. Mrs. Anastasia Mouskou – Peck, Lecturer of English and Technical Report Writing in the General Studies Department, attended **"Conference for Lifelong Learning"** which took place in Stirling, Scotland, 22 – 24 June 2007.

5. Dr Costas Neocleous, Senior Lecturer in the Mechanical Engineering Department and Chairman of the Central Academic Council, attended a short course in **"Compliant Mechanism Design"** at Massachusetts Institute of Technology (MIT) – Professional Institute, USA, 9 – 12 July 2007.

Visits/ Educational Exchange Programmes

1. Dr Nicholas Kathijotes, Lecturer in the Civil Engineering Department, visited the Poushkarov Institute under the Staff Exchange Programme, Sofia, Bulgary, 16 – 22 November 2006.

2. Dr Marinos Ioannides, Lecturer in the Computer Studies Department, visited the National Technical University of Athens within the Erasmus – Socrates Programme where he gave lectures, Athens, 15 – 19 January 2007.

3. Dr Kyriacos Kalli, Lecturer in the General Studies Department, participated in the Staff Exchange Programme and visited Aston University, Birmingham, UK, 22 – 26 January 2007.

4. Dr Marios Kassinopoulos, Lecturer in the Electrical Engineering Department, participated in the meeting of the National Coordinators of the European Programme "Socrates" which took place in Brussels, Belgium, 25 – 27 January 2007.

5. Dr Christos Marouchos, Lecturer in the Electrical Engineering Department, visited Brunel University under the Staff Exchange Programme where he gave lectures in **Module Power Electronics and FACTS**, UK, 20 – 26 February 2007

6. Dr Soteris Kalogirou, Instructor in the Engineering Practice Department, visited the London South Bank University within the Erasmus – Socrates Programme where he gave lectures, UK, 27 – 29 March 2007.

7. Mr. Sotos Voskarides, Lecturer in the Electrical Engineering Department, participated in the Erasmus – Socrates Programme and visited Orleans University where he gave lectures in **Electronic Subjects**, France, 2 – 6 April 2007.

8. Mr. Savvas Savvides, Head of the Engineering Practice Department, visited the Institute of Engineering and Technology and Clamorgan University, where he gave a lecture about **"The Evolving Higher Education System in Cyprus"**, London, 11 – 14 June 2007.

9. Mr. Charalambos Chrysafiades, Senior Lecturer in the Electrical Engineering Department visited the Technological Educational Institute of Thessaloniki, Greece, 11 – 15 June 2007.

10. Mr. Klitos Anastasiades, Lecturer in the Civil Engineering Department, participated in the Staff Exchange Programme and visited the Technological Educational Institute of Thessaloniki, where he gave lectures on **AutoCAD**, Greece, 11 – 15 June 2007.

11. Mr. Ioannis Demetriou, Lecturer in the Electrical Engineering Department, visited Tours University (IUT) where he gave lectures, France, 18 – 22 June 2007.

12. Dr Nicholas Kathijotes, Lecturer in the Civil Engineering Depa-rtment, visited the Kosice University under the Staff Exchange Programme, where he gave lectures about the **"Environmental Projects in Cyprus"**, Slovakia, 28 June – 4 July 2007.